



DOI: 10.5281/zenodo.1297163

CRITICAL ASSESSMENT OF CHROMATIC INDEX IN ARCHAEOLOGICAL CERAMICS BY MUNSELL AND RGB: NOVEL CONTRIBUTION TO CHARACTERIZATION AND PROVENANCE STUDIES

Bratitsi, M¹., Liritzis, I.¹, Vafiadou, A.¹, Xanthopoulou, V.², Palamara, E.³, Iliopoulos, I.²,
Zacharias, N.³.

¹*University of the Aegean, Lab. of Archaeometry and Lab. of Environmental Archaeology,
1 Demokratias Str, Rhodes 85132, Greece*

²*University of Patras, Dept of Geology, University Campus, Rio 26504, Greece*

³*University of Peloponnese, Dept of History, Archaeology and Management of Cultural Resources,
Lab of Archaeometry, Kalamata, Greece*

Received: 21/03/2018

Accepted: 29/07/2018

Corresponding author: Ioannis Liritzis (liritzis@rhodes.aegean.gr)

ABSTRACT

Hundred twenty archaeological ceramics (potsherds, figurines, stirrup jars) as well as experimental briquettes made from local clays fired at different temperatures were examined for their color index chromatic scale. Color was measured on clean surfaces, clearly fine decoration layers, from the Late Mycenaean settlement at Kastrouli, Central Greece. The aim is to critically assess these quantitative attributions of a color index to ceramic surfaces which depends on several factors, such as the type of clay, firing regime, subjective evaluation, lighting conditions. Our endeavor and aim are to classify groups of similar color that may imply same firing conditions and clay sources. The color perception within a chromatic context is investigated and the effect of light on color appearance is assessed. Indeed, apparent subjective differences in Munsell color evaluation, the sensitivity of chosen surface area and photo shooting setting under different light conditions are observed. Initially the evaluation of different color components, e.g. R, G, B; Lab; HSB, were examined using stereoscopic images as well as a mini digital micro USB microscope and edit with image processing software. Finally, the 3D plots and statistical clustering of RGB as average integrated and separate values with associated standard deviation error produce groups of similar ceramics compared to the briquettes. Results were corroborated by cluster analysis of R, B, G of sherds and fired clays.

KEYWORDS: Munsell, RGB, ceramics, photoshop, optical spectra, color, provenance, briquettes

1. INTRODUCTION

The characterization and provenance of ceramics and raw materials is a well-established procedure in archaeometry (Javanshah, 2018; Gajić-Kvaščevet al 2012; Papageorgiou & Liritzis 2007). It involves chemical and mineralogical analysis by physical methods (e.g. XRF, XRD, thin sections PLM, PIXE, ICP, NAA) and data evaluation through multivariate statistical methods (e.g. cluster analysis or dendrograms with various clustering algorithms, PCA biplots and 3D plots) (Matzourani & Liritzis 2006; Baxter, 2003). Such studies provide information on the extension of the territory exploited by ancient groups during the historical and prehistorical periods and contribute to the knowledge of long-distance circulation and exchange of raw materials and goods, hence on the *chaînes opératoires* of lithic and clay artefacts. Indeed, reconstructing mobility patterns is a major goal of researchers interested in prehistoric societies and the use of geochemical source characterization of ceramics found at sites in a region, offers a way to reconstruct the procurement range – local in close proximity, travelled long distances or trade exchange – by prehistoric groups to obtain resources. Either way reflects major issues concerning their development, independency and identity of settlements compared to other major centers.

Pottery, due to its remarkable storage capability, was a vital item used in the food activities of everyday life. But ceramic artifacts too had a valuable intangible meaning (e.g. figurines). Not only these uses, but aesthetic qualities, too, were frequently used by people. Ceramics are also preferred materials in provenance studies as their physico-chemical properties are most often different at a major, minor but mainly trace element level, because of their mode of formation from characteristic clay sources.

The soils, i.e. the clayey raw materials are classified according to the way they were formed, the nature of their impurities and their behavior during firing, and these are the factors that determine their final color. This color may be the same throughout the ceramic, but at the same time there is the phenomenon where the core is dark, while the outer and/or internal appear to be light in color because of the firing time, which is insufficient for full maturation of its mass, thus forming two or three different color levels.

The present study proposes a radically different approach of grouping and provenance of ceramics and raw materials, using chromatic (optical) means, a successful attempt which was made as a case study on materials derived from Kastrouli (Fig.1,2) Late Mycenaean (Late Helladic III) settlement at Desfina near Delphi, Central Greece (E37° 54 19.56, N42° 50 792.35).

(A)



(B)



Figure 1. (A) View towards Kastrouli hill from Aghia Eirini slope. In red arrow the site, (B) from Kastrouli view to Aghia Eirini/ Xenophon clay sources (note whitish/yellowish colors across the valley).

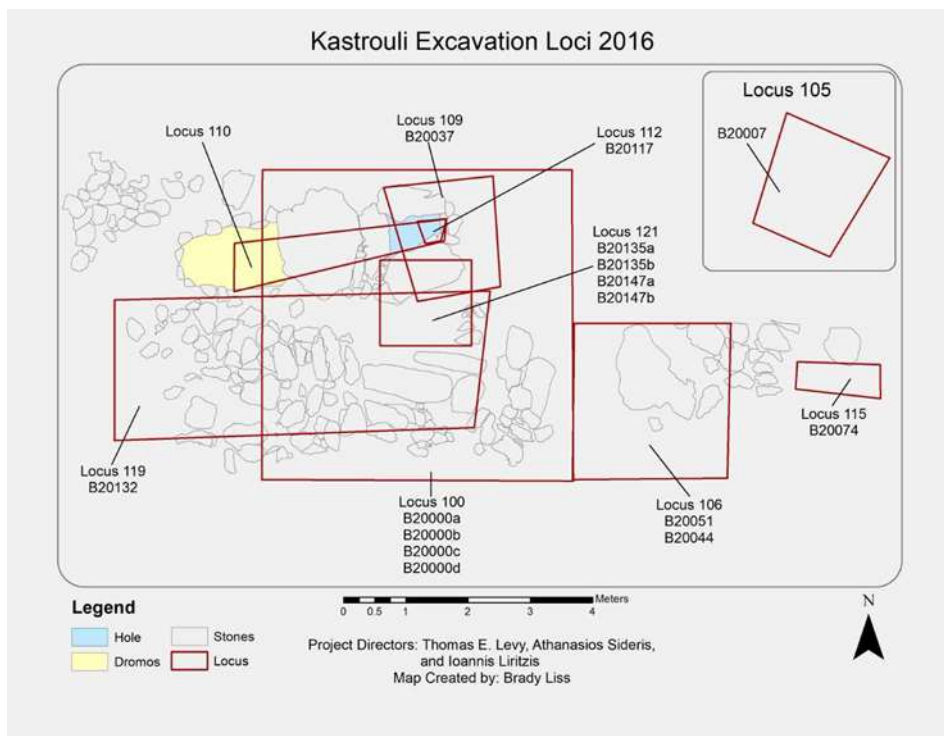


Figure 2. Locus of excavated ceramics at Kastrouli (from Liritzis et al 2018)

It is a common practice to use the chromatic index of Munsell scale, a routine method of making a first sorting of the color of the ceramic material, as simple, easy, cost effective, and timely manner, method. This contains a numerous of chromatic differences which are individualized with code groupings and it is applied to ceramics. At any rate, it is obviously an extremely subjective approach not avoiding the error-prone and time-consuming procedure of Munsell

Estimation by visual means and without any expensive tool. This has been improved by the automatic recognition of color method (Milotta et al., 2017) though the noise reduction is cumbersome and further algorithms are needed for clay, and experimental fired clays compared to the ceramics.

In the present research, the Munsell color was estimated by four users, whereas new methods were proposed. That is, the RGB (for Red, Green, Blue)

scale, the intensity and the spectra, as well as the luminosity and other color components. During the process of color determination through RGB indexes strict regulations were followed concerning the capture images, the choice of the surface area of the materials and the light settings. The processing of data and images was made via image processing software. Biplots and Cluster analysis (dendrograms) corroborated this approach.

2. MATERIALS, METHODS AND INSTRUMENTATION

2.1 *Ceramics and Clayey Raw Materials*

A typological representative set of 127 ceramic sherds (potsherds, figurines, stir-up jars) originate from the Kastrouli excavations (Fig. 2), including some fired clays from the floor was chosen (Table 1) (Sideris *et al.*, 2017; Levy *et al.*, 2018). They all date in the Late Mycenaean III (1300-1150 BC) (Liritzis *et al.*, 2018a).

TABLE 1: *Ceramic identification*

sherd	Description	
K1-K5	diagnostic sherds K3 = handle of coarse ware large shape, K5 = base(?) of fine-walled small shape, probably LH (Late Helladic)	
K6	group I diagnostic pottery	
K7	large pithoi sherd, bulk pottery	
K8	diagnostic pottery	
K9-K14	Diagnostic Pottery, Bulk Pottery, Lumpy Clay?	Three are non-diagnostic. Two are coarse ware handles, and two fine ware handles. One is a base of a large shape, and one a rim of a small shape - fine ware. The fine ware is LH; the coarse ware may be LH or later.
K15-K17	ceramic	
K18-K20	stirrup jars	
K21-K29	bulk pottery diagnostic	
K30-K31	bases	Five shards of fine ware, four of coarse ware and one probably a wall- or floor-revetment clay fragment. Again the fine ware seems LH, the coarse ware may be from the same period or later.
K32-K40	bulk pottery	
K41-K56	diagnostic pottery	All fine ware and LH. K56 - K66 very fine, from stirrup jars, and small alabastra or three-handled amphorae. Some sherds may belong to stirrup jars.
K57-K62	Pottery with Pigment, Diagnostic Pottery, and Bulk Pottery	
K63-K81	diagnostic sherds	
K82-K83	bulk pottery	
K84	pithos	Two coarse ware sherds from large shapes; five fine ware sherds from stirrup jars and cups (from cups are the reddish sherds K85 and K87), LH.
K85	Diagnostic and Bulk Pottery	
K86-K87	diagnostic pottery / pottery w / pigment	
K88	???	
K89	Pottery with Pigment, Diagnostic Pottery	
K90		Three shards from LH stirrup jars.
K91	Pottery with Pigment, Diagnostic Pottery, and Bulk Pottery	
K92	special pottery	
K93	diagnostic pottery	Four shards from stirrup jars and one from a cylindrical alabastron, all LH.
K94	Pottery with Pigment, Diagnostic and Bulk Pottery (intact base and body of a vessel)	
K95	Diagnostic Pottery (Stirrup jar spout and 4 fragments of the same jar)	
K96	???	
K97	Pottery with Pigment, Diagnostic Pottery	
K98	Pottery with Pigment, Diagnostic Pottery, 1 sherd from same vessel?	All fine ware; three non-diagnostic shapes; three from stirrup jars. The diagnostic are all LH.
K99	Pottery with Pigment, Diagnostic Pottery (Rims?)	

K100-K102	Pottery with Pigment, Diagnostic and Bulk Pottery	
K103	???	
K104	???	
K105	figurine	All figurines are LH in date.
K106	figurine	
K107	figurine	
K108	figurine	
K109	figurine	
K110	special pottery	Four handles of alabastra or other shapes; two sherds from stirrup jars; one foot of a cup, all LH. Fragment of a clay loom-weight (K111, clay yellow), presumably also LH.
K111	loom weight	
K112	Diagnostic Pottery	
K113		
K114		
K115	Pottery with Pigment, Diagnostic Pottery, and Bulk Pottery	
K116	Diagnostic and Bulk Pottery	
K117	Pottery with Pigment, Diagnostic Pottery, and Bulk Pottery	
K118-K120	Diagnostic Pottery	
K121	conical bead	
K122	Lumpy Clay	
K123-K126	large pithos sherd, bulk pottery	
K127	Coarse ware sherd of a large shape, probably a pithos, with inclusions, which seem to be from ground pottery. It may be from LH to Hellenistic, but earlier dates (LH or Geometric) are more probable.	

The ancient ceramic and clayey sediments were photographed in the visible optical spectrum and a clean (avoiding decoration and any deposition) surface was selected. The images recorded are shown in

Fig.3, including some significant artifacts the psi and phi type figurines (Fig. 4). The complete sequence of the sherds is given in **Appendix 1** - Fig. A1).



Figure 3 Macro- photographs of all ceramics analyzed. In appendix photos of all sherds are included



Figure 4: Figurines K105-K108 of front and back sides, and K109 piece of a phi base.

Additionally, Experimental briquettes were made with local raw material and fired at different temperatures (700, 900 and 1050°C). These temperatures were chosen aiming to cover (i) the possible temperature regime which was applied by the ancient potters and (ii) the mineralogical reactions which take place and affect the end color of the ancient ceramics. All the clay sources are located in the vicinity of the site (Fig.1A and Table 2).

The clay-rich sediments were coarsely ground, mixed with tap water and left to soak a few days. Excess water was removed, and the clays were left to dry to a workable state, at which point three briquettes were prepared from each sample. The briquettes were left to dry for a week at room temperature and subsequently were fired at 700°C, 900°C and 1050°C, respectively, in a Vulcan 3-550 box furnace with programmable controls. Firing took place under oxidizing conditions, at a rate 8°C/min, with

the maximum temperature (soaking time) held for 6 hours. The briquettes were let to cool overnight in the furnace with the door closed and left at room temperature for at least one week, allowing any lime re-hydration a chance to develop so as to observe its impact on the fabric consistency (Fig. 5A).

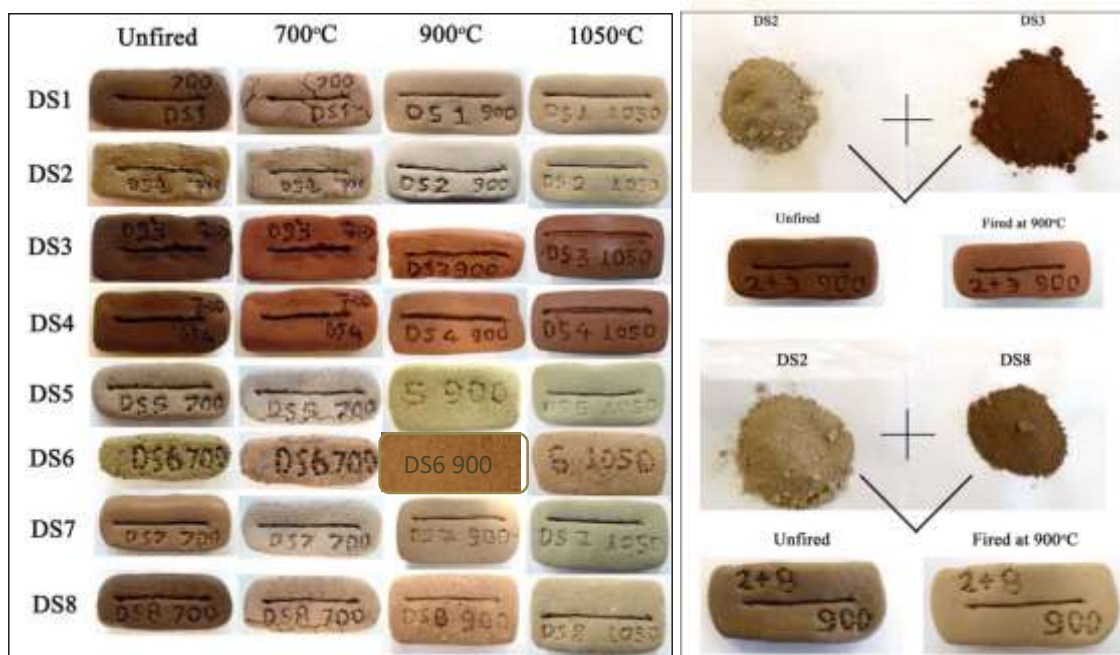
Experimental briquettes were made as well, after mixing the clayey sediments (DS2+DS8 and DS2+DS3) and were fired at 900°C and under oxidizing regime. Mixing was based upon their different chemical composition and according to pXRF analysis (Liritzis *et al.*, 2018b), DS8 is characterized as calcareous sample (CaO=63.68 wt%), whereas DS2 and DS3 are characterized as non-calcareous (CaO=2.76 wt% and CaO=4.87 wt%, respectively). Thus, the first mixing was performed using 3 parts of DS2 and one part of DS8, whilst for the second one 2 parts of DS2 were mixed with 3 parts of DS3 (Table 2, Fig.5B).

TABLE 2. Clay sources in the vicinity of the settlement, firing temperature, color and comments.

Clay code Numbers	Location	Firing temperature, °C	Color after firing	Comments
DS1	Aghia Eirini	700, 900, 1050	Whitish-yellowish	Chapel of St. Irene and presence of water reservoir. The location is called <i>Asprojia</i> by locals due to whitish color of sediments
DS2	Aghia Eirini	700, 900, 1050	Whitish-yellowish	Chapel of St Irene and presence of water reservoir
DS3	Limnos	700, 900, 1050	Brown	Called <i>limnos</i> as during winter forms a lake-like pod
DS4	Meteles	700, 900, 1050	Brown	Like Limnos accumulates water during winter and in a distance of ~300 m from Kastrouli. The name

				<i>Meteles</i> means half implying the other half of the valley of Desfina.
DS5	Aghia Eirini-Xenophon	700, 900, 1050	Whitish	Along the path from <i>Xenophon</i> location (west of Aghia Eirini) towards Aghia Eirini
DS5c	Xenophon			Tile found on surface near the well.
DS6	Aghia Eirini - Xenophon path	700, 900, 1050	Pale yellow	Aghia Eirini-Xenophon path
DS7	Xenophon	700, 900, 1050	Light grey	<i>Xenophon</i> location is close to the presence of a well for water storage (tank ~10 m deep and 1.5-2 m width variable from top to bottom). The age of the well is unknown but older than 200-300 of years.
DS8 (another sample)	<i>Meteles</i>	700, 900, 1050	Light brown	Like Limnos accumulates water during winter and in a distance of ~300 m from Kastrouli. The name means half implying the other half of the valley at Desfina. DS8 is characterized as calcareous sample (CaO=63,68 wt%),
DS2+ DS8		900		Mixing DS2: DS8= 3:1
DS2+DS3		900		DS2 and DS3 are characterized as non-calcareous (CaO=2.76% and CaO=4.87% respectively). Mixing DS2:DS3= 1:1.5

All sources come from location around Kastrouli hillock, the closest walking distance is in the south the *Meteles*, then in the north Aghia Eirini and Xenophon, and are well seen from the site. Along the path between Xenophon - Aghia Eirini we observe three (3) chromatic deposits - whitish, pink, yellowish. Photos were taken. The Aghia Eirini and Xenophon samples were collected from banks of local torrents. Sampling was performed after removal of the superficial layers.



(A)

(B)

Figure 5 (A) Briquettes coded DS of the local clay sediments of Desfina fired at temperatures at 700, 900 and 1050 °C, (B) mixed clays fired at 900 °C.

In the present investigation we used the briquettes of 900°C and 1050°C as the sherds derive from small size ceramics whose firing time ranges mainly around these temperatures. The larger and voluminous pots were usually fired in outdoor kilns, where temperatures can hardly exceed 800-850 °C.

2.2 Methods & Instruments

Four tools were tried; namely Munsell color chart, photoshop, microscopic observation and cluster analysis.

a. Munsell chromatic chart

The Munsell soil-color charts (2009 year revised, 2013 production date, 2017 purchased date) were used to classify the color index. The Munsell scale for color consists of separate notations for hue, value and chroma, which are combined in that order to form the color designation. The symbol for hue is the letter abbreviation of the color of the rainbow, R for Red, YR for Yellow-Red, Y for Yellow, preceded by numbers from 0 to 10. The notation for value consists of numbers from 0, for absolute black, to 10, for absolute white, and for chroma consists of numbers from 0 for neutral gray and increasing at equal intervals to a maximum of 20. (Soil Survey Manual 1951).

Comparison of the color of the sherd is obtained by holding it directly behind the color chip under daylight conditions. It is rare to find a perfect match, so the sample's color will be determined by the closest match.

Four different users and readings were applied by Maria and Asimina (B.M. and V.A., Lab. of Archaeometry, University of the Aegean), Vayia (X.V., Research Lab. of Mineral and Rocks, Department of Geology, University of Patras) and Eleni (P.E., Lab. of Archaeometry, University of Peloponnese) (see, Appendix, Table A1).

It is observed that the users selected different chromatic index in several cases (Table 3), which makes the application of the Munsell scale doubtful, and requires attention. The lighting of the room is extremely important. Monitoring with natural light is preferred, because clay color as well as Munsell scale alters in naked eye. However, disadvantages arise in terms of the subjectivity of the results and the difficult conditions (satisfactory light, sun lighting etc).

Indeed, from Table 3 it is concluded that the subjectivity of the Munsell color scale efficiency creates a critical non-precarious effect in the next interpretation. Thus, alternative scientifically sound approaches were devised here based on the use of RGB under strictly controlled shooting conditions.

b. Adobe Photoshop

Photoshop is an image processing professional software of Adobe (edition cc 2014) that uses different chromatic models which were employed in our trials (e.g. R, G, B; Lab; HSB) as described below. Since Munsell measurements consist of three attributes of color: hue (color appearance parameters), value (Luminosity), and chroma (color purity), and each pixel of the images consists of a triad of colors; Red, Green and Blue, hence the chromatic model initially tried was the RGB. Thus, it was decided to remain in the triad of R, G, B of a quantitative nature

compared with 3Dcluster diagrams. The Photoshop RGB color mode uses the RGB model and assigns an intensity value to each pixel. In 8-bits-per-channel images, the intensity values range from 0 (black) to 255 (white) for each of the RGB (red, green, blue) components in a color image. RGB images use three colors, or *channels*, to reproduce colors on screen and the RGB model is used by computer monitors to display colors.

Subsequently, we used another chromatic model offered by photoshop, the *Lab* (L stands for Luminosity that can range from 0 to 100; a component (green-red axis), and *b* component (blue-yellow axis) can range from +127 to -128). The CIE $L^*a^*b^*$ color model (*Lab*) is based on the human perception of color. Because *Lab* describes how a color looks rather than how much of a particular colorant is needed for a device (such as a monitor, desktop printer, or digital camera) to produce colors, *Lab* is considered to be a device-independent color model. Color management systems use *Lab* as a color reference to predictably transform a color from one color space to another. Finally, since Munsell measures hue, value and chroma, we tried a 3rd triad, the HSB (Hue, Saturation and Brightness).

c. Microscopic Observations

For introducing the sherds surface areas in the photoshop and measure their chromatic models, the shooting areas on ceramic surface should have been representative and clear. Due to inhomogeneity of the measured ceramic sherds inherited by xenoliths, mixing, colors and accretion, stereoscopic images obtained via a Stereoscope MODEL Zeiss Discovery V.8 varied significantly. Despite of the effort to obtain comparable shooting conditions, the external lighting, the difference in the relief, gave results which are not commensurable to each other. Thus, the obtained surface images were alternatively acquired via a USB microscope (DigiMicro USB Microscope 1.3Mpix), from surface areas and from the sectioned profiles of the already broken pieces of sherds found in situ. All shootings were taken in full darkness, and the plastic case of the microscope rests slightly on the surface (so there is no fear of damage to the ceramics). The conditions of obtaining images were defined and measurable for comparison. The distance between surface area and the lens is variable due to focus purposes, the LEDs intensity was low (instrument's first scale), with no external lighting present and the area photographed was specific each time.

d. Cluster Analysis

The hierarchical clustering is based on the connectivity of the basic concept of data that is most relevant to the nearby elements rather than to the more

distant ones. It consists of a whole group of methods that differ to the way distances are calculated. The user must decide which connection criterion to use, since a cluster consists of multiple elements, there are several options for calculating the distance. These methods will not produce a unique separation of the dataset, but a hierarchy from which must select the appropriate clusters that are depended by their distance. In this study, Euclidean distance or Euclidean metric is used which is the "usual" straight line between two points in the Euclidean space. With this distance, Euclidean space measures the minimum distance between the two points in the level. The result produced is based on finding nearest pairs of points with the minimum distance between a larger set of points (Baxter 2003). The Mahalanobis distance was also used to measure the distance between a point P (fired clay at certain temperature) and a distribution (an identified group from cluster analysis of ancient ceramics).

Generally, any clustering approach poses a risk because the data are three variables, very closely re-

lated, so it's like having a clustering problem with 1 variable. At any rate this gives an indicative correlation useful for the present case.

3. THE MEASUREMENTS

3.1 The samples and various tentative color measurements

A total of 127 ceramic fabric images have been processed. These photos were shot by Canon camera (Canon EOS 1200D) and macro lens (EF-S 18-55mm). The macro photos helped to distinguish the clean spots from those containing impaction or other differentiations, from the pure color of the pottery. Subsequently, a first classification was made based upon the Munsell chromatic scale.

The Munsell chromatic index was applied by four different users on same areas of each ceramic. An example of the Munsell attribution is given in Fig.6. The results of all ceramic finds in a excel format (Table A1, in Appendix) and were grouped (Table 3).

TABLE 3. Attribution of color using Munsell scale by four users for chromatic and associated sub-grouping of same chromatic efficiency. Bold indicates coincident occurrences among two or more users.

2.5YR (Hue)					
Color	Value/Chroma	Maria	Asimina	Eleni	Vayia
Pinkish white	8/2	K49, K50	-	-	-
Light reddish gray	7/1	K4 (inner) , K7(inner)	K4 (inner)	-	-
Light reddish brown	6/4	K89	-	-	-
Light red	7/6	K51(inner), K109		K96	-
	6/6	K70(margin) , K95	K2(margin), K61(margin), K70(margin) , K100(margin)	K98	
	6/8	K61(inner), K88 , K100(inner) , K125	-	K100(margin)	K16(inner), K72, K85, K88 , K99, K100(margin) , K125
Dark reddish gray	4/1	-	-	-	K100(inner)
Reddish brown	5/4	-	-	-	K1(margin)
Red	5/6	K6(margin)	-	-	-
	5/8	-	-	-	K2(margin), K35(margin), K61(margin), K82, K118(margin)
	4/6	-	-	-	K101

5YR (Hue)					
Color	Value/Chroma	Maria	Asimina	Eleni	Vayia
White	8/1	K57, K97	-	-	-
Pink	8/4	-	-	-	K90
	7/4	K1(inner), K12 , K30(margin), K58, K96, K105	K2(inner), K11	K12 , K74, K75	-

Pinkish gray	7/2	-	K38	-	-
	6/2	K30(inner)	-	-	-
Light red-dish brown	6/3	K41, K110(inner)	-	-	-
	6/4	K2(inner), K11, K35(inner), K36, K74, K75 , K98, K99, K108	K5, K12, K29(margin), K36, K37, K54, K74	K54	K2(inner), K36 , K41, K75
Reddish yellow	7/6	K13 , K37, K40, K52, K53, K54, K119(margin)	K13 , K14, K30(margin), K32(margin), K82, K89, K104, K119(margin)	K11, K51(inner), K108, K109	K5, K13 , K14, K29(margin), K30(margin), K54 , K55, K109
	7/8	K82	-	-	K13
	6/6	K2(margin), K5, K14, K16(inner), K22(margin) , K34, K39, K59(inner) , K62, K72 , K78, K85, K104	K22(margin) , K34, K39 , K40, K55(inner), K59(inner) , K60, K62, K72 , K88, K95, K101 , K109	K2(inner), K5, K14, K22(margin), K55(inner), K62 , K70(inner), K72 , K89, K95, K101	K12, K22(margin) , K37, K40, K51(margin), K55(margin), K60 , K74, K89, K104 , K119(margin)
	6/8	K10(margin), K118(inner)	K85	K61(inner), K85, K88	K34, K39, K62, K70(inner), K78, K95
Gray	5/1	-	-	-	K61(inner)
Reddish brown	5/3	K35(margin), K107	K118(margin)	-	-
	5/4	-	-	-	K6(margin), K123(margin)
Yellowish red	5/6	K38 , K60, K101	-	K60	K38 , K59(inner)
	5/8	-	-	K34, K36, K37, K38	K10(margin)
Dark gray	4/1	K6(inner) ,	K6(inner) , K100(inner)	-	-

7.5YR (Hue)					
Color	Value/Chroma	Maria	Asimina	Eleni	Vayia
Pinkish white	8/2	K33(margin)	K90	-	-
Pink	8/3		K30(inner)	K103	
	8/4	K90, K112	-	K90, K112, K120	K7(margin), K27, K73(margin), K112
	7/3	K17, K48	K1(margin), K17, K42, K48, K52, K70(inner), K71	K58, K91	K1(inner), K4(margin), K17, K24
	7/4	K15 , K27, K29(margin), K44, K46, K55(margin), K63 , K71, K83, K91, K92 , K94, K102, K103 , K113 , K120	K9, K15 , K27, K44, K46, K53, K58, K63 , K91, K92 , K93, K99, K102, K103 , K112, K113 , K119(inner)	K9, K15 , K17, K27, K44, K48, K53, K55(margin), K63 , K65, K70(margin), K71, K92 , K93, K105	K15 , K16(margin), K21, K26, K42, K48, K53, K58, K63 , K67, K92 , K127(margin)
Reddish yellow	7/6	K32	K94	K94, K102, K106, K107, K113, K119(inner)	K9, K11, K91, K93, K94, K96, K98, K102, K113
	6/6	K26(inner), K43, K122	K43, K78	K13, K32(inner), K39, K43 , K59(inner), K78, K82, K104, K122	K25(margin), K32(margin), K43 , K122
	6/8	-	-	K40	-
Pinkish gray	6/2	-	K75	-	-
Light brown	6/3	-	K28 , K41	K28	-
	6/4	K9, K21 , K24, K26, K42, K65 , K93, K106	K21 , K24, K26, K55(margin), K65 , K96, K98, K122	K16(inner), K21 , K26, K41	K3(inner), K28, K46, K65, K86
Gray	5/1	-	-	-	-
Brown	5/3	K86	K125	-	-

	5/4	K28, K126	K35(inner), K110(margin)	-	K126
Strong brown	5/6	-	-	K110(margin)	-
	4/6	-	-	-	K4(inner)

10YR (Hue)					
Color	Value/Chroma	Maria	Asimina	Eleni	Vayia
White	8/1	-	K76	K97	
Light gray	7/1	-	-	K4(inner), K33(margin)	K127
	7/2	K31, K67	K18, K19 , K20, K32(inner), K51(inner), K68	K19	K7(inner)
Very pale brown	8/3	K20 , K77, K117	K81, 114	K20 , K68, K87	K18, K45, K64, K114, K116
	8/4	K114	-	K77, K114, K117	K77, K80, K87, K97, K117, K120
	7/3	K7(margin), K19, K68, K81, K87 , K115, K116	K8, K77, K87 , K116, K127(inner)	K1(inner), K18, K30(inner), K52, K56, K67	K52, K56, K123, K127(inner)
	7/4	K84 , K127(inner)	K84 , K120, K124	K29(inner), K81, K84 , K124	K8, K19, K20, K33(margin), K47(inner), K68, K71, K81, K84 , K115, K124
Yellow	7/6	K111	K111	K111	-
Gray	6/1	K118(margin)	K1(inner), K126	-	-
	5/1	-	K73(inner)	-	K110(inner)
Light brownish gray	6/2	K10(inner)	K47(inner), K123(inner)	-	-
Pale brown	6/3	K3(inner) , K8, K18, K70(inner)	K3(inner) , K10(inner), K29(inner)	K3	-
Light yellowish brown	6/4	K47(inner), K124	-	K8, K10(inner), K24, K42, K46, K123(inner)	K103, K110(margin)
Brownish yellow	6/6	-	-	-	K111
Brown	5/3	K3(margin)	-	-	-
Yellowish brown	5/4	K123(inner)	-	K125	-
Dark gray	4/1	K100(margin)	-	-	-
Dark grayish brown	4/2	-	-	-	K59(margin)

2.5Y (Hue)					
Color	Value/Chroma	Maria	Asimina	Eleni	Vayia
White	8/1	-	K25(inner), K79, K97	-	-
Light gray	7/1	-	K7(inner) , K31, K33(inner), K118(inner)	K7(inner) , K127(inner)	K32(inner)
	7/2	-	K57, K66, K69, K115	K47(margin), K69	K31
Pale brown	8/2	K23, K66, K80	K23, K49, K50	K31, K49, K57, K64, K66, K76, K79, K115	K57, K79
	8/3	K45	-	K50, K80	K49, K69, K76
	8/4	-	-	K45	K66
	7/3	K69, K79	K80	K23	-
Gray	6/1	-	K61, K83, K86	K22(inner)	K35(inner), K83
	5/1	-	K110(inner)	K35(inner), K61(margin),	K73(inner)

				K73(inner), K86, K110(inner), K126	
Light brownish gray	6/2	-	-	K25(inner), K118(inner)	K47(margin), K118(inner)
Dark gray	4/1	-	-	K6(inner), K100(inner)	K6(inner)

5Y (Hue)					
Color	Value/Chroma	Maria	Asimina	Eleni	Vayia
Light gray	7/1	K25(inner), K33(inner)	-	-	-
	7/2	-	-	-	K51(margin)
Gray	6/1	K22(inner)	K22(inner)	K83	K25(inner)
	5/1	-	K16(inner)	-	-
Dark gray	4/1	-	K121	-	-
Olive gray	4/2	K121	-	-	K121

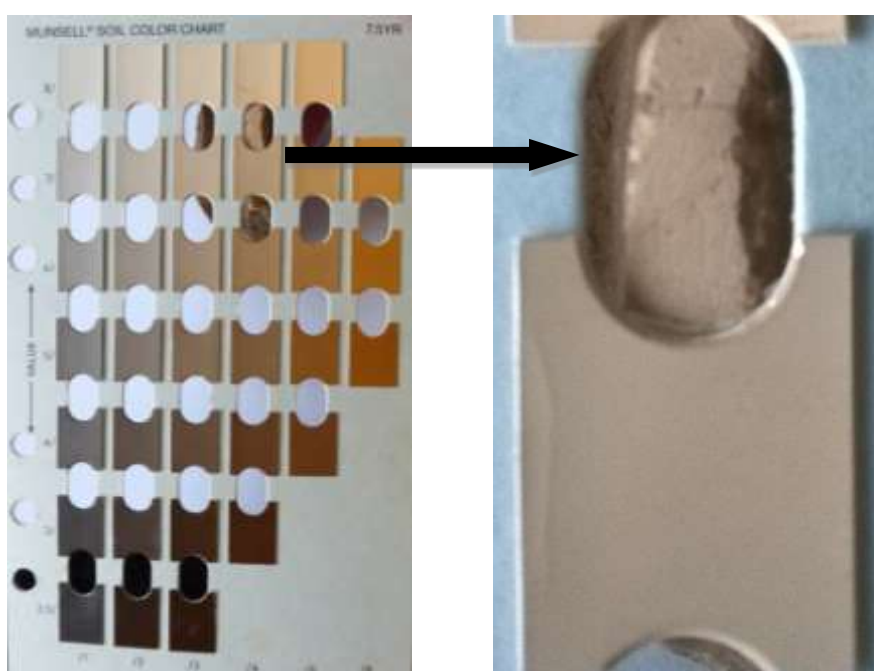


Figure 6. Ceramic K92, corresponds to 7.5YR 7/4 (the lower color scale is the correct one).

The color scale grouping revealed the large differences between readings by the users (in Table 3 bold font indicates the common measurements), due to purely subjective causes implied mainly by the eyesight and lighting environment.

The Munsell color scale was followed by photography of ceramics using stereomicroscopy (Stereoscope MODEL Zeiss Discovery V.8) and a first attempt was made measuring the color from the histogram of Adobe Photoshop CC 2014 for each color element (Fig.7).

All tests made referred to small (focused dashed rectangular) and clean areas (Fig.8).

The values of R, G and B, as well as Luminosity, were measured (Fig.8). Tests were also made on several color elements for each sherd on a focused spot. In particular, Lab (Luminosity L (0-100), *a* (colour scale -128 bluish to +127 pinkish magenta), *b* (-128 blue to +127 yellow)), as well as HSB (Hue, Saturation and Brightness), were measured (Fig.9).

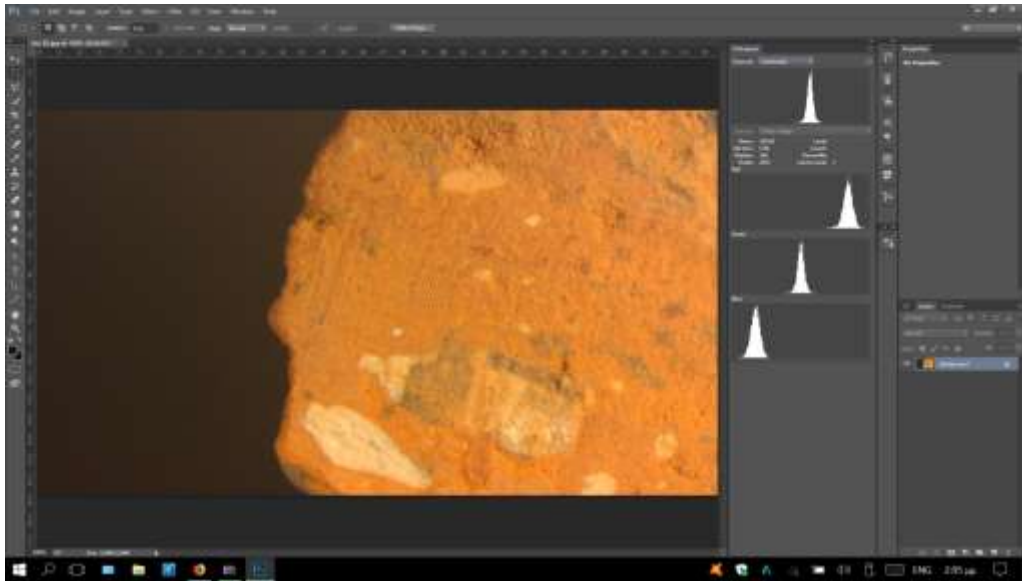


Figure 7: The image of ceramic surface K82 from the histogram of Adobe Photoshop CC 2014 for each color element

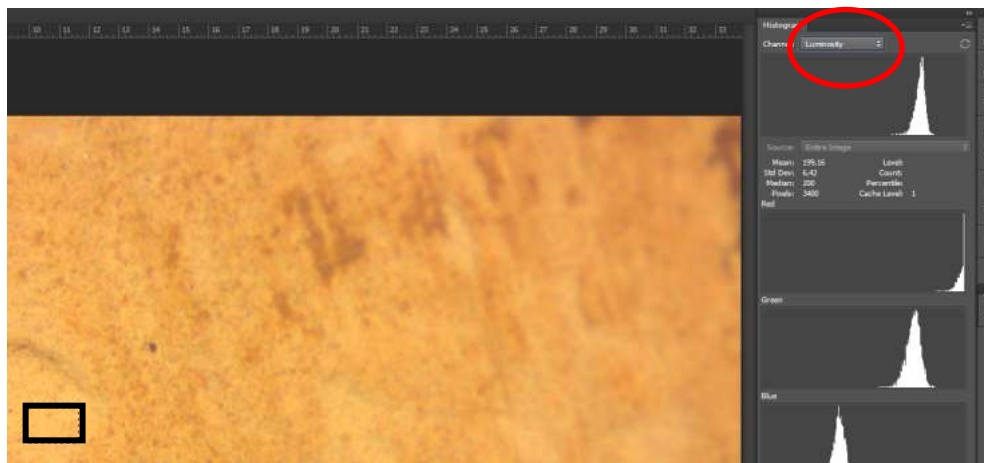
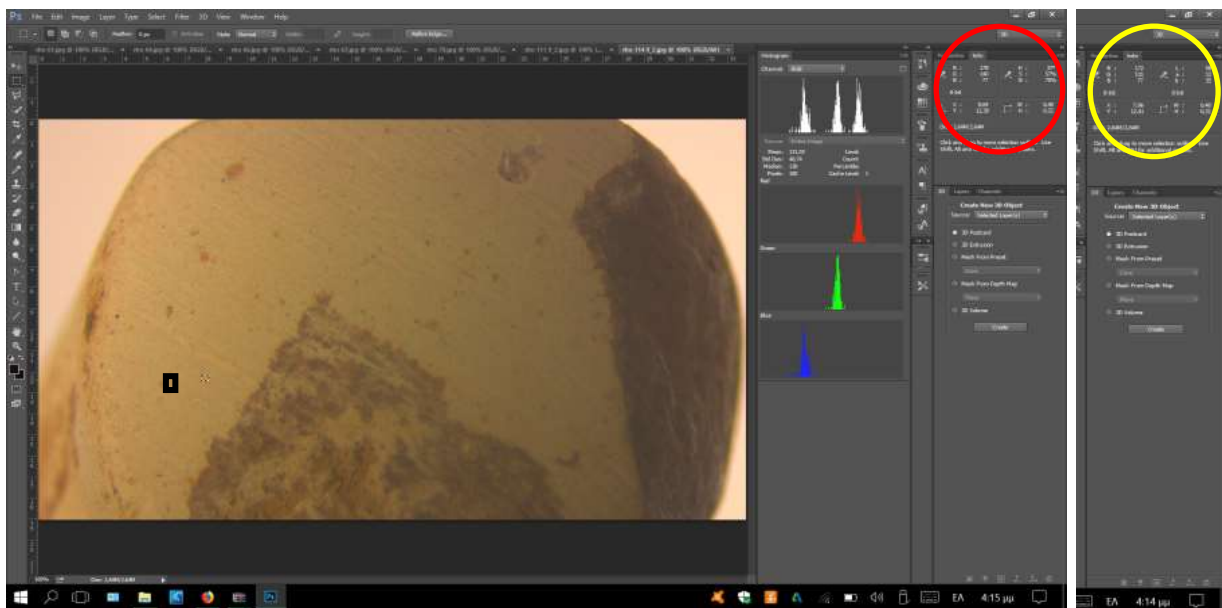


Figure 8. R, G, B and Luminosity measured on focused rectangular sub-areas, values given in right white spectra.



Lab HSB

Figure 9. Measured values of Lab (red circle) and HSB (yellow circle) of a representative surface sub area.

3.2 3D plots

Subsequently, the R, G, B triads individual data were used for 3D cluster (with OriginPro 9.0) and further promising results were obtained as they matched with the grouping given by Munsell and refer only to the chromatically similar sherds (e.g. K82 and K85 all readings are congruent belonging to

the same group) (Fig.10A). Also, groupings were obtained by the 3D cluster of triads Lab (Fig.10B) and HSB (Fig.10C). The latter trial gave no conclusion, due rather to the drastic variations of measured parameters in adjacent points around the chosen small areal spot.

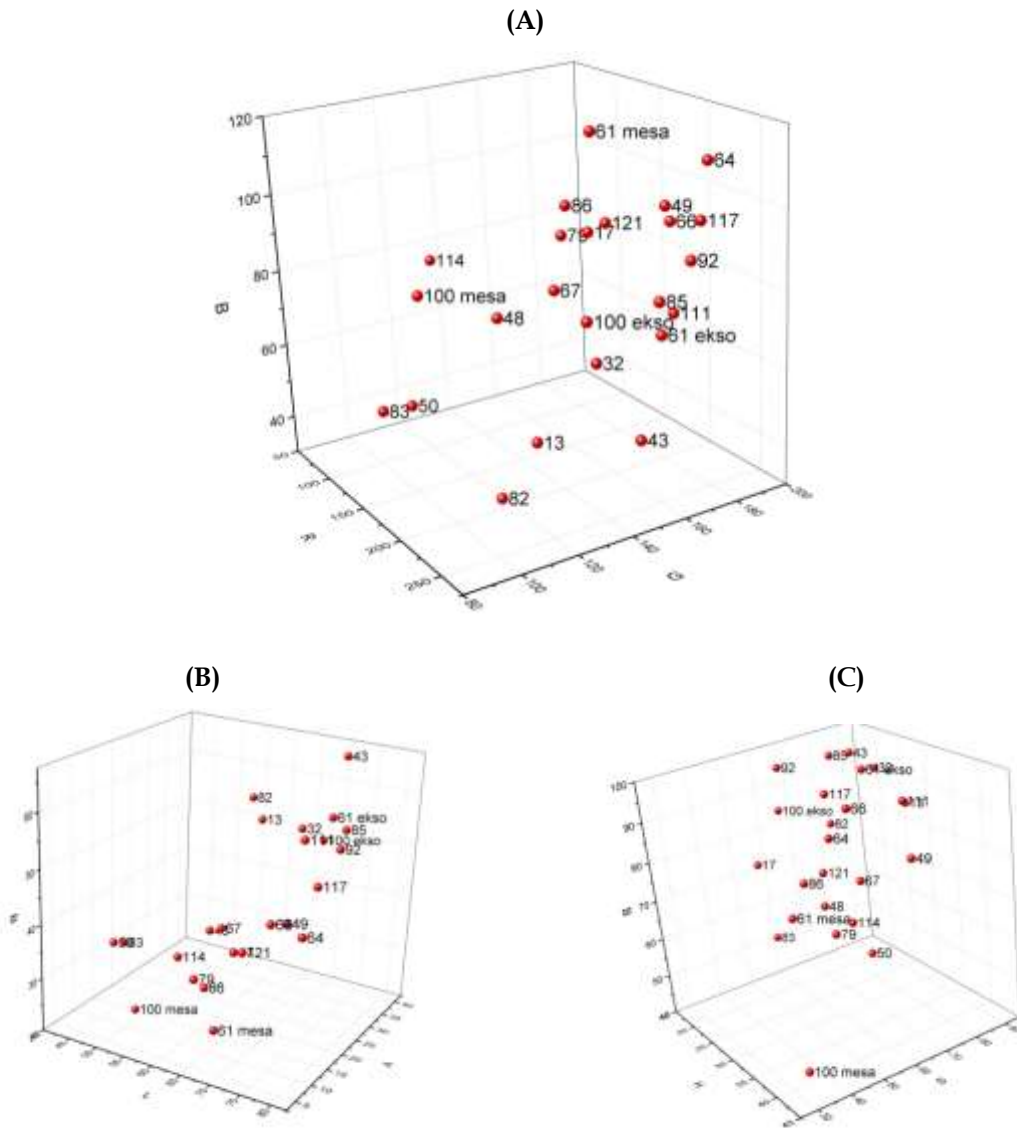


Figure 10. 3D cluster of triads (A) R,G,B; (B) L, a, b, (C) H, S, B,

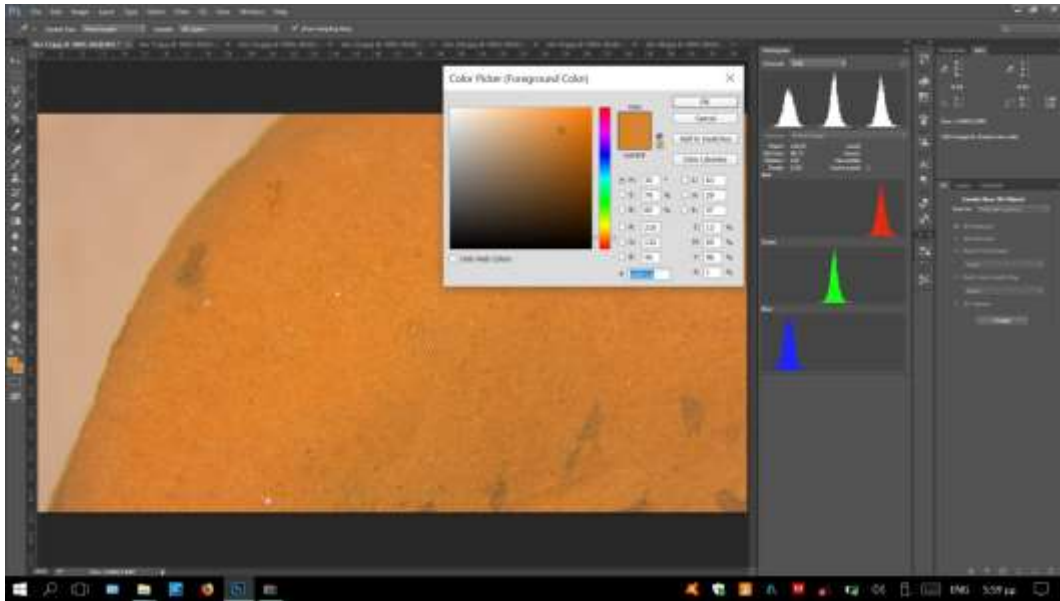


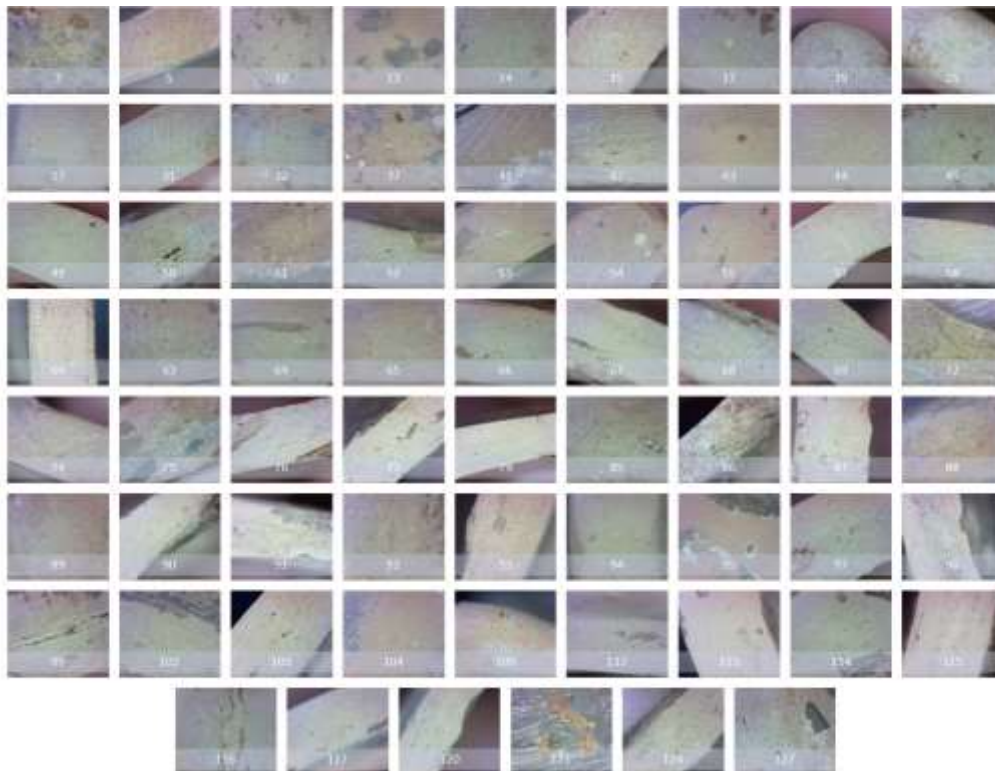
Figure 11. Colour picker via photoshop on pointed spots.

Another attempt using colour-picker via Photoshop on pointed spots did not either produce concluded convergence (Fig.11), due to subjectivity of colour estimation.

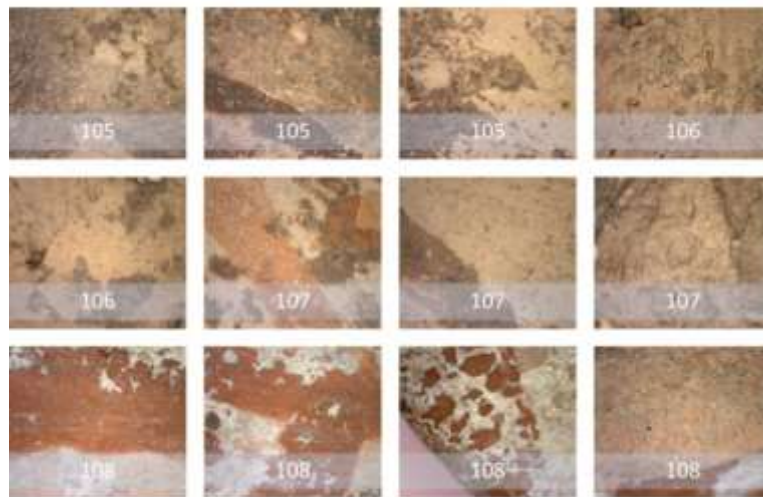
Since great differences have been observed which were attributed to the changes in the shooting conditions of the stereoscope, such as, distance from object surface but mostly photo shading, we gave an effort to avoid them and turn to USB microscope readings.

3.3 USB digital microscope images

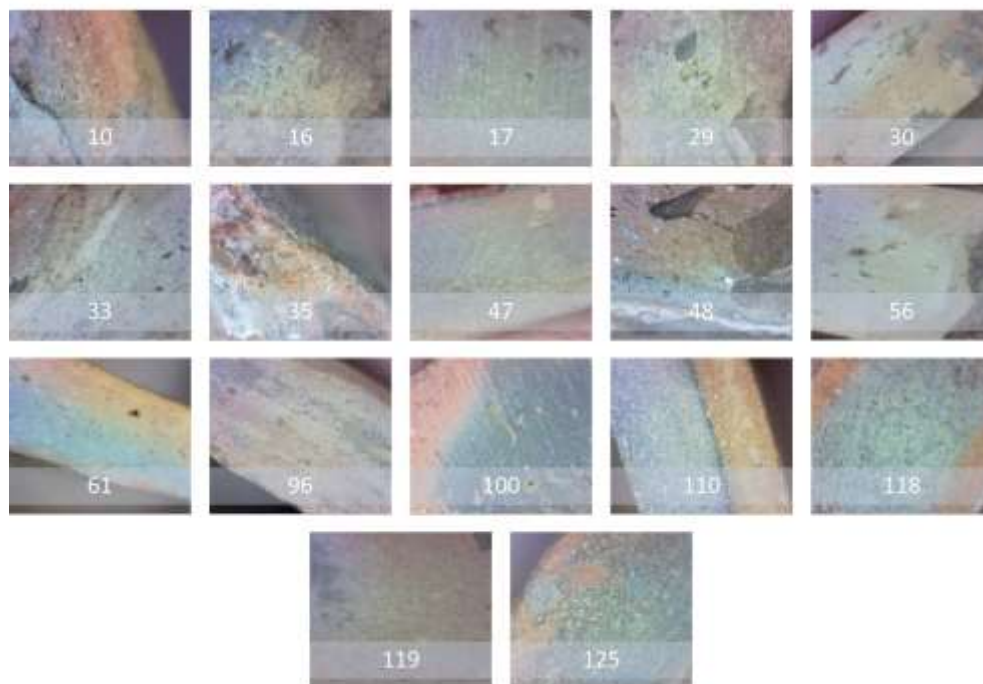
The images obtained with USB microscope (DigiMicro USB Microscope 1.3 Mpix) were those taken under the most standardized conditions during this study because: 1) the distance to the object was kept the same, 2) any external light intrusion was preventive since the images were taken in totally dark room having as light only the microscope's LEDs, whose intensity was at low scale in order to avoid the surface solarization (Fig.12).



(A)



(B)



(C)

Figure 12. Images taken with the USB microscope from: (A) the ceramic sherds; (B) the four figurines; and (C) ceramics with a chromatic change (two to three colors) in the inner and outer layers. Shooting of different areas are shown (white numbers refer to code numbers of respective ceramics).

The 3D plotting (OriginPro 9.0) of separate Red, Green, Blue (RGB) intensities for all are given in Fig.13. (NB: Biplot projections of R, B, G of the 3D diagrams of ceramics and briquettes are given in Fig.A2 of the Appendix).

It is of great interest to particularly observe the sherds with single profiled surfaces throughout the

ceramic (Fig. A2) with those with difference in inner and outer profile, as well as, the briquettes and figurines with similar behavior. Therefore, the results focused on 99 sherds (Fig.12A), the 3 figurines (K105-K107), and only two of the briquettes which were sandwiched-formed while fired (DS3, DS4).

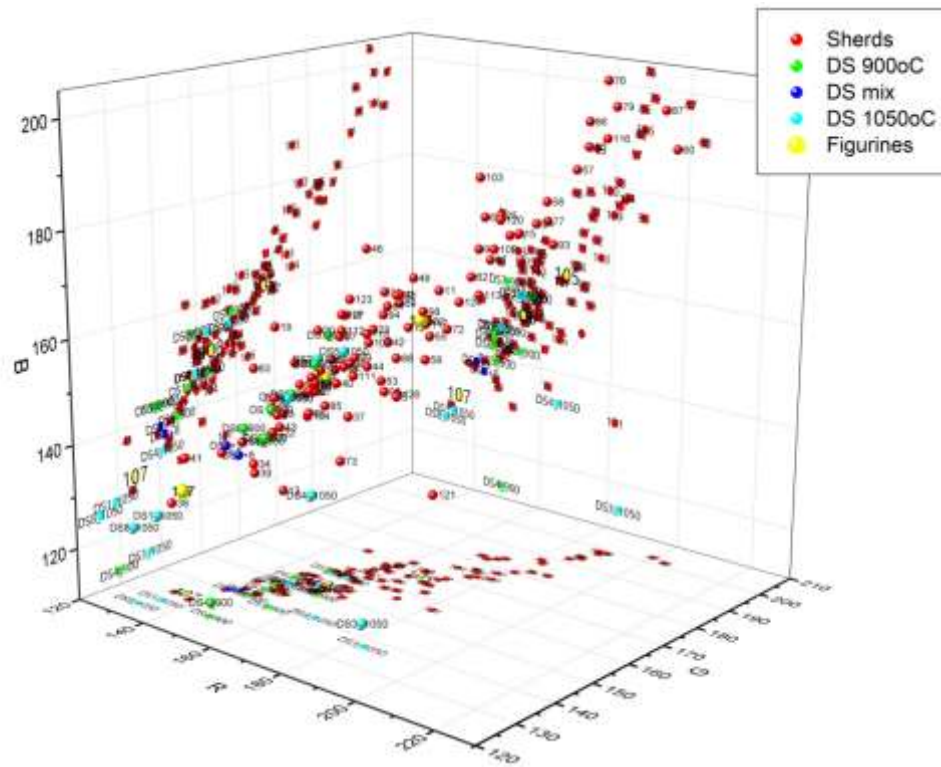


Figure 13. 3D grouping of RGB's of clean ceramics, figurines and briquettes (900 °C -1050 °C and mixed at 900°C).

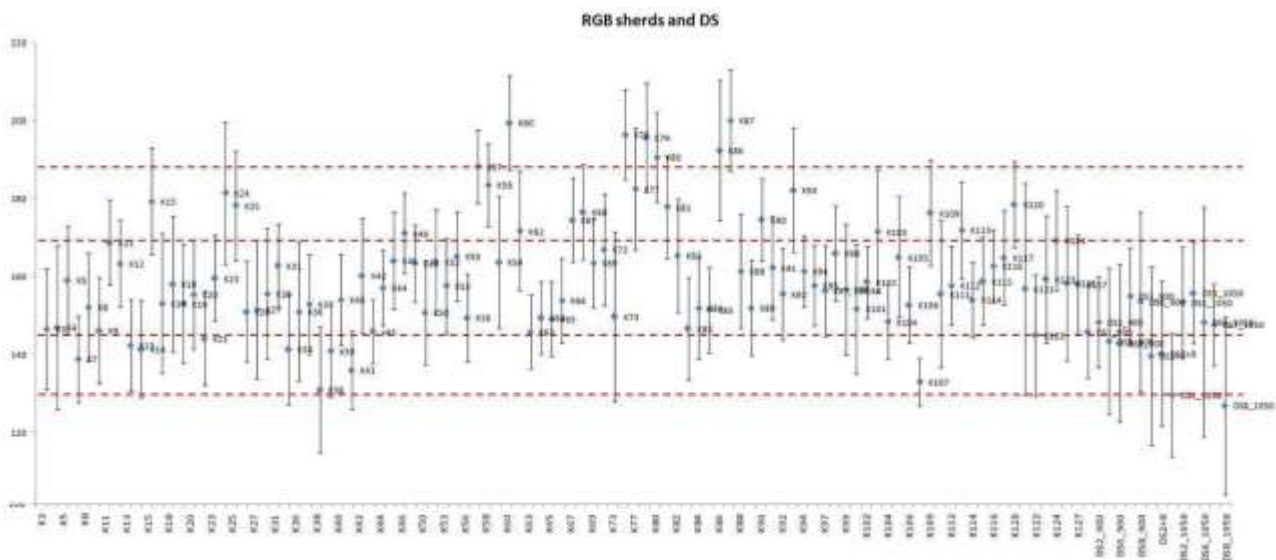


Figure 14. The analyzed clay objects and fired clays as a function of their integrated RGB spectral intensity.

3.4 Statistical analysis: Biplots and Hierarchical Clustering

The integrated RGB with associated error bars for each reading of ceramics sherds were also plotted as bi-plot, and promising groupings were observed (Fig.14). The fired experimental briquettes were also included (code DS in Fig. 14 and Table 4).

This first test revealed four zones of groups within their error bars; 130-145, 145-170, 170-190, and >190 (Table 4). These are compared with cluster analysis of Fig. 15 and Tables 5A, B. This initial grouping interestingly enough is somehow commensurate with the Cluster analysis (further neighbor method, squared Euclidean).

Table 4. Tentative grouping of 99 ceramics and DS fired clays of integrated RGB values from the biplot (Fig.14A). Bold numbers are those in marginal limit between 2 adjacent groups and are placed in the closest one.

Group1: 130-145	Group 2: 145-170	Group 3: 170-190	Group 4: >190
K7, K13, K14, K38, K39, K41, K107(figurine), DS1(900oC) , DS2(900oC) DS2+3(900 oC), DS2+8(900oC), DS1(1050oC), DS6(1050 oC) , DS7(1050oC) , DS8(1050 oC)	K3, K4, K5, K8, K9, K12, K16, K18, K19, K20, K21 , K23, K26, K27, K28, K31, K34 , K36, K37, K40, K42, K43, K44, K49, K50, K53, K56, K63, K64, K65, K66, K69, K73, K83, K84, K85, K89, K92, K94, K95, K97, K99, K101, K102, K104, K106(figurine), K111, K112, K114, K115, K116, K117, K121, K122 , K123, K126, K127 DS5(900oC) , DS6(900oC) , DS7(900oC), DS8(900oC), DS2(1050oC), DS5(1050oC)	K11 , K15, K24, K25, K45 , K46, K52 , K55 , K58, K59 , K62, K67, K68, K72 , K77, K81, K82 , K88 , K90, K91 , K98 , K103, K105(figurine) , K109(figurine), K113, K120, K124	K57 , K60, K76, K79, K80, K86, K87 , K93

The measured R, G, B data were also processed by statistical analysis using StatGraphics Plus 5.0 and R for measuring distances of similarity namely, the cluster analysis (dendrograms) employing *complete linkage (or furthest neighbor)*, where the distance between two clusters is the distance between their two most distant members, and *average linkage* compromise method under which the distance between two clusters is the average of the distances of all pairs of observations, one observation in the pair taken from the first cluster and the other from the second cluster. Both indicate relevant and worth examining groupings (Fig.15).

The ceramic and clay data were processed first separately and then combined, but the results

change radically in terms of clustering even for the ceramics themselves. The most appropriate approach is to group the ceramic set of data, and then using the Mahalanobis distance to classify the additional observations (clay data set) in some of the groups that have already been identified. Another way is to cluster ancient sherds and modern fired DS clays as one data set, since both are homogeneous.

The Cluster Analysis (CA), complete and average linkage, for 99 ceramics sherds is presented in Fig.15. The analysis revealed three groups (Table 5). Regarding the accompanied statistical data are given in **Appendix – TablesA2, A3**.

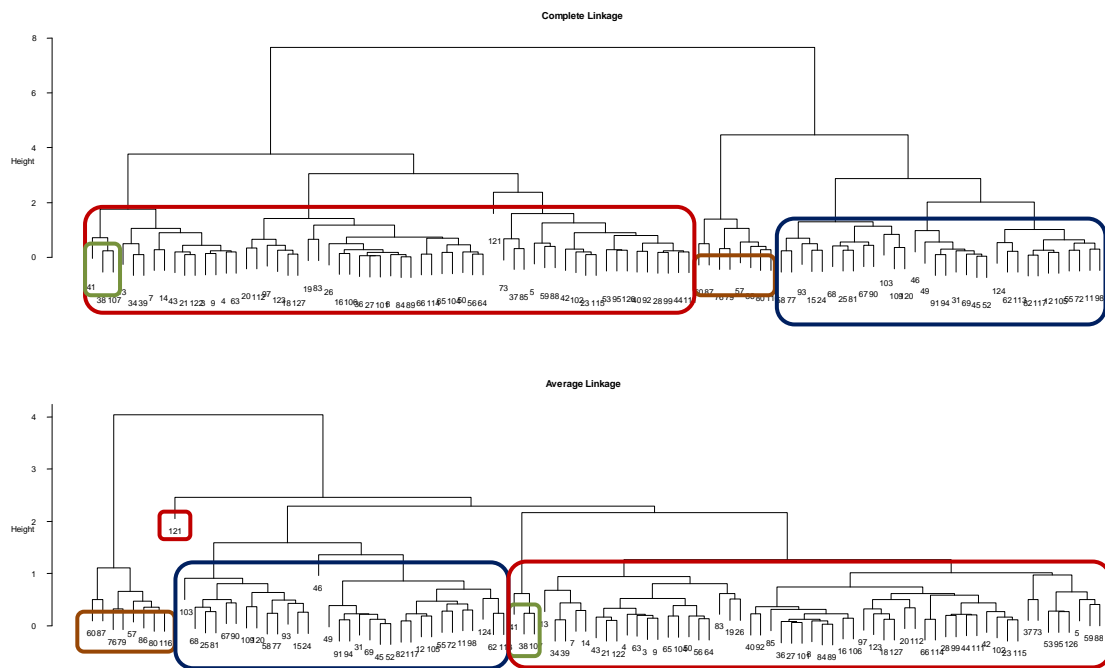


Fig.15 Clustering of ceramics and clays with R software. Clustering (complete and average linkage) of clean surface ceramic sherds and figurines. Colors indicate the three identified groups, group 1 red, group 2 blue, group 3 brown. With green are outlined the three sherds marginally belonging to group 1. Sherd 121 is steatite conical bead.

Table 5A: Cluster analysis of average and complete linkage of 99 ceramic sherds using R software (excluding sand-wiched ones). The identified groups in red, blue and brown areas of Fig.15. The marginal samples are in green and in red is the outlier steatite conical bead.

Group 1 (red)	Group 2 (blue)	Group 3 (brown)
K3 K4 K5 K7 K8 K9 K13 K14 K16 K18 K19 K20 K21 K23 K26 K27 K28 K34 K36 K37 K38 K39 K40 K41 K42 K43 K44 K50 K53 K56 K59 K63 K64 K65 K66 K73 K83 K84 K85 K88 K89 K92 K95 K97 K99 K101 K102 K104 K106(figurine) K107(figurine) K111 K112 K114 K115 K121 K122 K123 K126 K127	K11 K12 K15 K24 K25 K31 K45 K46 K49 K52 K55 K58 K62 K67 K68 K69 K72 K77 K81 K82 K90 K91 K93 K94 K98 K103 K105(figurine) K109 K113 K117 K120 K124	K57 K60 K76 K79 K80 K86 K87 K116

Table 5B: EXCELL Cluster analysis of complete linkage of 99 ceramic sherds and DS clays using Statgraphics software. The four identified groups (1-4) from the RGB biplot of Fig. 14 and the other four (C + DS) from the results of CA (furthest neighbor). Grouping assignment is identical for the two first groups of each approach (Groups 1 and 2 are similar to 1C+DS and 2C+DS, respectively).

Sample No	Group1	Group2	Group3	Group4	1C+DS	2C+DS	3C+DS	4C+DS
1	1	1	1	1	1	1	1	1
2	2	2	2	2	2	2	2	2
3	3	3	3	3	3	3	3	3
4	4	4	4	4	4	4	4	4
5	5	5	5	5	5	5	5	5
6	6	6	6	6	6	6	6	6
7	7	7	7	7	7	7	7	7
8	8	8	8	8	8	8	8	8
9	9	9	9	9	9	9	9	9
10	10	10	10	10	10	10	10	10
11	11	11	11	11	11	11	11	11
12	12	12	12	12	12	12	12	12
13	13	13	13	13	13	13	13	13
14	14	14	14	14	14	14	14	14
15	15	15	15	15	15	15	15	15
16	16	16	16	16	16	16	16	16
17	17	17	17	17	17	17	17	17
18	18	18	18	18	18	18	18	18
19	19	19	19	19	19	19	19	19
20	20	20	20	20	20	20	20	20
21	21	21	21	21	21	21	21	21
22	22	22	22	22	22	22	22	22
23	23	23	23	23	23	23	23	23
24	24	24	24	24	24	24	24	24
25	25	25	25	25	25	25	25	25
26	26	26	26	26	26	26	26	26
27	27	27	27	27	27	27	27	27
28	28	28	28	28	28	28	28	28
29	29	29	29	29	29	29	29	29
30	30	30	30	30	30	30	30	30
31	31	31	31	31	31	31	31	31
32	32	32	32	32	32	32	32	32
33	33	33	33	33	33	33	33	33
34	34	34	34	34	34	34	34	34
35	35	35	35	35	35	35	35	35
36	36	36	36	36	36	36	36	36
37	37	37	37	37	37	37	37	37
38	38	38	38	38	38	38	38	38
39	39	39	39	39	39	39	39	39
40	40	40	40	40	40	40	40	40
41	41	41	41	41	41	41	41	41
42	42	42	42	42	42	42	42	42
43	43	43	43	43	43	43	43	43

44	44	44	44	44	44	44	44	44
45	45	45	45	45	45	45	45	45
46	46	46	46	46	46	46	46	46
47	47	47	47	47	47	47	47	47
48	48	48	48	48	48	48	48	48
49	49	49	49	49	49	49	49	49
50	50	50	50	50	50	50	50	50
51	51	51	51	51	51	51	51	51
52	52	52	52	52	52	52	52	52
53	53	53	53	53	53	53	53	53
54	54	54	54	54	54	54	54	54
55	55	55	55	55	55	55	55	55
56	56	56	56	56	56	56	56	56
57	57	57	57	57	57	57	57	57
58	58	58	58	58	58	58	58	58
59	59	59	59	59	59	59	59	59
60	60	60	60	60	60	60	60	60
61	61	61	61	61	61	61	61	61
62	62	62	62	62	62	62	62	62
63	63	63	63	63	63	63	63	63
64	64	64	64	64	64	64	64	64
65	65	65	65	65	65	65	65	65
66	66	66	66	66	66	66	66	66
67	67	67	67	67	67	67	67	67
68	68	68	68	68	68	68	68	68
69	69	69	69	69	69	69	69	69
70	70	70	70	70	70	70	70	70
71	71	71	71	71	71	71	71	71
72	72	72	72	72	72	72	72	72
73	73	73	73	73	73	73	73	73
74	74	74	74	74	74	74	74	74
75	75	75	75	75	75	75	75	75
76	76	76	76	76	76	76	76	76
77	77	77	77	77	77	77	77	77
78	78	78	78	78	78	78	78	78
79	79	79	79	79	79	79	79	79
80	80	80	80	80	80	80	80	80
81	81	81	81	81	81	81	81	81
82	82	82	82	82	82	82	82	82
83	83	83	83	83	83	83	83	83
84	84	84	84	84	84	84	84	84
85	85	85	85	85	85	85	85	85
86	86	86	86	86	86	86	86	86
87	87	87	87	87	87	87	87	87
88	88	88	88	88	88	88	88	88
89	89	89	89	89	89	89	89	89
90	90	90	90	90	90	90	90	90
91	91	91	91	91	91	91	91	91
92	92	92	92	92	92	92	92	92
93	93	93	93	93	93	93	93	93
94	94	94	94	94	94	94	94	94
95	95	95	95	95	95	95	95	95
96	96	96	96	96	96	96	96	96
97	97	97	97	97	97	97	97	97
98	98	98	98	98	98	98	98	98
99	99	99	99	99	99	99	99	99
100	100	100	100	100	100	100	100	100
101	101	101	101	101	101	101	101	101
102	102	102	102	102	102	102	102	102

103	103	103	103	103	103	103	103	103
104	104	104	104	104	104	104	104	104
105	105	105	105	105	105	105	105	105
106	106	106	106	106	106	106	106	106
107	107	107	107	107	107	107	107	107
108	108	108	108	108	108	108	108	108
109	109	109	109	109	109	109	109	109
110	110	110	110	110	110	110	110	110
111	111	111	111	111	111	111	111	111
112	112	112	112	112	112	112	112	112
113	113	113	113	113	113	113	113	113
114	114	114	114	114	114	114	114	114
115	115	115	115	115	115	115	115	115
116	116	116	116	116	116	116	116	116
117	117	117	117	117	117	117	117	117
118	118	118	118	118	118	118	118	118
119	119	119	119	119	119	119	119	119
120	120	120	120	120	120	120	120	120
121	121	121	121	121	121	121	121	121
122	122	122	122	122	122	122	122	122
123	123	123	123	123	123	123	123	123
124	124	124	124	124	124	124	124	124
125	125	125	125	125	125	125	125	125
126	126	126	126	126	126	126	126	126
127	127	127	127	127	127	127	127	127
DS1-900	DS1-900	DS1-900	DS1-900	DS1-900	DS1-900	DS1-900	DS1-900	DS1-900
DS2-900	DS2-900	DS2-900	DS2-900	DS2-900	DS2-900	DS2-900	DS2-900	DS2-900
DS5-900	DS5-900	DS5-900	DS5-900	DS5-900	DS5-900	DS5-900	DS5-900	DS5-900
DS6-900	DS6-900	DS6-900	DS6-900	DS6-900	DS6-900	DS6-900	DS6-900	DS6-900
DS7-900	DS7-900	DS7-900	DS7-900	DS7-900	DS7-900	DS7-900	DS7-900	DS7-900
DS8-900	DS8-900	DS8-900	DS8-900	DS8-900	DS8-900	DS8-900	DS8-900	DS8-900
DS2+3	DS2+3	DS2+3	DS2+3	DS2+3	DS2+3	DS2+3	DS2+3	DS2+3
DS2+8	DS2+8	DS2+8	DS2+8	DS2+8	DS2+8	DS2+8	DS2+8	DS2+8
DS1-1050	DS1-1050	DS1-1050	DS1-1050	DS1-1050	DS1-1050	DS1-1050	DS1-1050	DS1-1050
DS2-1050	DS2-1050	DS2-1050	DS2-1050	DS2-1050	DS2-1050	DS2-1050	DS2-1050	DS2-1050
DS5-1050	DS5-1050	DS5-1050	DS5-1050	DS5-1050	DS5-1050	DS5-1050	DS5-1050	DS5-1050
DS6-1050	DS6-1050	DS6-1050	DS6-1050	DS6-1050	DS6-1050	DS6-1050	DS6-1050	DS6-1050
DS7-1050	DS7-1050	DS7-1050	DS7-1050	DS7-1050	DS7-1050	DS7-1050	DS7-1050	DS7-1050
DS8-1050	DS8-1050	DS8-1050	DS8-1050	DS8-1050	DS8-1050	DS8-1050	DS8-1050	DS8-1050

Table 6: Mahalanobis distances for each of the DS samples from the three groups of the ceramics (when treated alone). Samples DS3, DS4 produced sandwiched briquettes when fired and are not considered here.

	Group 1	Group 2	Group 3
DS1_900	0.8218790	14.685390	234.6006
DS2_900	1.6399934	10.316952	184.7747
DS5_900	1.3200585	18.574452	279.8853
DS6_900	3.1257738	25.283049	331.8666
DS7_900	2.9755259	5.971697	123.6577
DS8_900	5.5389305	19.571710	270.9760
DS2+3	2.8183776	23.533937	309.0458
DS2+8	2.4987329	22.300356	306.8247
DS1_1050	9.7406350	42.274221	461.5488
DS2_1050	1.1079793	11.152805	197.9726
DS5_1050	0.8762524	5.299095	143.9307
DS6_1050	0.3095314	12.796774	222.0971
DS7_1050	0.5665883	12.534591	214.0191
DS8_1050	12.6633152	49.643588	514.3485

Prompting to classify the clays, (DS samples) fired at different temperatures, in one of the three groups of ceramics (revealed when these are treated alone), the Mahalanobis distances for each of the DS samples from the three groups is calculated (Table 6).

From Table 6 it is observed that all DS samples belong to Group 1 with higher probability (Mahalanobis distance values less than 5), and the DS7_900, DS5_1050 and DS2_900 could be also fit into Group 1 though may well be in Group 2 (Mahalanobis less than about 10). The DS2_1050 marginally belongs to Group 2 and it does not belong to Group 3.

Compared to the CA complete linkage of ceramics and DS clays (Fig.14), the identified four groups are shown (Table 5B) with some similarity.

Comparing RGB biplot with CA and Mahalanobis distance test it appears that: groups 1& 2 from Fig.14 (biplot) is commensurable with group 1 of Fig.15 (by CA); the group 3 of Fig.14 (biplot) similar with group

2 of Fig.15 (by CA); and group 4 of RGB biplot similar to group 3 of CA in Fig.15.

4. DISCUSSION

The CA of the grouping of R, B, G' s of ceramics alone compared to fired clays from Desfina plain (DS), and the CA of both sets treated as one, revealed three and four groups, respectively. The integrated RGB revealed four groups.

Through the two statistical approaches the 3rd group (Group 3) established when the sherds are treated alone is similar to the 4th group (ie. 4C+DS) revealed when sherds and fired clays are treated together. The samples assigned to the first two groups (Group 1 and Group 2) when the sherds are treated alone, are scattered in three groups (1C+DS; 2C+DS; 3C+DS) when the fired clays (DS samples) are included in the data set (see Table 5B). Obviously, the differentiation of groupings has to do with the statistical treatment; in one case Mahalanobis distance compared to ceramic sherds and in the other the further neighbor method applied to one set including DS and sherds.

The four groups established through the biplot of integrated RGB seems to reach a satisfactory yet not strictly coincident correspondence with the CA of sherds + DS together.

The grouping of ceramics and provenance study inheres risky factors for drawing lightly solid conclusions. The preparation of clays from raw materials presents some variations in: a) major element composition, and, b) color from firing temperature. The present investigation of the chromatic index and use of RGBs to group ceramics led us to reconsider issues of methodology for characterization, comparison and provenance studies.

The four groups of integrated RGB of ceramics implies use of local clays (either single sources or mixed of two in our current trial) for two groups of ceramics; those of 125-145 and 145-170 units (Fig. 14). Another group appears not to be related with the current clays sources analyzed. The latter implies either another local source not yet identified (there are some more in the area and in a walking distance from the settlement) or imported via trade.

At first inspection of the dendrograms, the grouped samples by CA appear chromatically also to follow these groupings, as well those formed in the integrated biplot of Fig14 (and Appendix Figs A2 and the 3D plot of Fig.13). In fact, in the integrated RGB biplot the high Ca content ceramics (K50, K83, K103) fall within the lower two groups of DS clays.

The XRF analysis (Liritzis *et al.*, 2018b in preparation) of fired local clays have had a high calcium content, at any rate they ranged between 2% to 72%.

The mixed clays still possess an increased Ca (24% and 56% respectively) and this apparently makes them to form a separate cluster. For example, K50, K83 and K103 have 18-27% of Ca close to DS clays. Yet, despite this high Ca content which certainly adds a variance to the groupings the DS2+3 and those of DS3 and DS 4 (Ca = 2-6%) fall better within a ceramic group, and the trace element clustering is clearly evident of the use of local clays. For example, DS4 and K3, K32, K43, K48 with low Ca content. More mixed proportions (with Ca in the range of 3-15%) in the future will verify this point.

The above remarks are supported by the first mineralogical – chemical investigations that the present groupings include fired clays and ancient ceramics, while a group of ceramics seems at present of unknown clay source (Xanthopoulou *et al.*, 2018 in preparation).

Some particular remarks are:

1) The B-G and R-G biplots in clean ceramic surface have a linearity, while for R-B a dispersion exists. Thus, the Green factor defines the hueing/dispersion,

2) The Green component is controlled by the type of clay and firing, 3) Among the DS in 1050°C only four fall within the ceramic group (DS2, 5, 6 and 7. NB: DS2: whitish, DS5: whitish, DS6: reddish, DS7: whitish)

The whitish clays are found in several locations around Kastrouli, the present ones derive from St Irene site called 'asproyia' (=whitish) by locals. The local clay sampling noted that the hueing of this whitish clay ranges from white to light pink or yellow. For the other clay locations, DS1 is very light brown, DS3 and DS4 become sandwich upon firing and DS8 is light brown. From DS fired in 900°C, the DS4 (Meteles) RGB intensity is medium to low, while in 1050°C the R increases and B, G are low.

In the mixed DS (DS3+2, DS2+8 at 900°C) both are low in the tail of the curve.

The DS 4 and DS 8, Meteles (close to Kastrouli), though from same location they have different behavior in the firing and color. This may imply different blend.

3) Close to the mixed DS are ceramics K34, 39, 7, 14, 41, with large error bars, due to high blend as evident from the microphotographs (mixed soils, small piece

4) We consider that the adjacent sherds in the linear distribution have similar behavior, color, firing temperature, surface deposits.

5) In the apparent linear curves we observe that those DS belonging to the linearity are in the lower parts of RGB:

- R: 130-200, DS =140-165

- B: 125-210, DS = 130-165
- G: 130-205, DS = 130-160

The RGB and other measurements of color in ceramic surfaces was a necessity due to the subjective and poorly defined yet very relative and with no sufficient value to use Munsell chromatic index.

Regarding the wavelength of each RGB color that in relation to the perception of eye is a question worth of further discussion. Hence, we adapt one particular model of what light conditions are typically like - here the USB microscopy - and we work from the multiple sensor readings to find the most probable readings under that model.

The settings, the cameras and all the procedure of taking images under the same conditions for all surface samples as described above. The light conditions are "typically" like varies a lot depending on the illumination (and on whether one records emission spectra or absorption spectra). The amount of energy reflected at a particular wavelength depends not only on the properties of the material but on the strength of the illumination at that wavelength. For non-monochrome unfiltered light the profile depends upon the temperature of the source.

It is worth noting that the output of RGB readings are not necessarily the same as the sensor readings, even if one is working with a set of three sensors that are most sensitive to red, green, and blue. The computations to go from sensor readings to RGB have to take into account details of the sensitivities and of course of the illumination model being used, and search for variables such as "illumination estimation", "illumination estimate", "illuminant estimate", etc.

Concerning the question of how the three monochrome-equivalent values for the R, G, B components relate to a single wavelength original, the answer is not unique. In short, one cannot know any wavelength per R, G, B.

Overall, the standard settings for taking images using our microscope and cameras, on a proportional way, despite a systematic shift that actually exists in comparison with other sensors and processing, provides a robust clustering technique for provenancing purposes.

ACKNOWLEDGEMENTS

We thank Ministry of Culture, Greece for providing the permit to analyze ceramic finds, Assoc Prof I. Pappageorgiou for contribution to R analysis and helpful comments and Prof. A. Sideris for some ceramic typology comments.

REFERENCES

Baxter, M.J. (2003) *Statistics in archaeology*. Arnold, London.

Attempts have been made at estimating the spectrum of colors in digital images (e.g. see Color and Imaging conference in the past: http://www.imaging.org/Site/IST/Conferences/CIC/C/CIC_Home.aspx?WebsiteKey=6d978a6f-475d-46cc-bcf2-7a9e3d5f8f82&hkey=d2cf3f19-87b4-4164-8274-c40180e9dfa7&CIC25_Sections=6#CIC25_Sections).

5. CONCLUSION

The proposed decision-making procedure whose goal is to classify unknown ceramic findings based on their elemental compositions derived by R, G, B chromatic values gives satisfactory results.

Munsell scale is a widely used method to inexpertly define color classification in ceramics but lacks reliability and objectivity.

Measuring other parameters (HSB, Lab) does not provide correct results or sufficient enough for color assessment. The RGB seems to inhere potential with promising results.

Measuring larger area in lieu of a point focus is after all indicative of the color, provided that the USB images are taken under similar conditions, same distance between USB microscope lens and ceramic

USB is preferred to stereoscope; for the latter lighting has greater dispersion.

Using a dark room is a very significant condition to avoid external inhomogeneities brought by the light. The result in general depends upon the size of the ceramic sherd, the degree of smoothness, any contaminations and clay additives, the schism during firing in the kiln.

The firing temperature, firing rate and duration in the kiln results to a variable burnt structure (homogeneous, sandwiched) and those should be separately examined for their color.

The firing is not indicative of the chromatic attribution and of the final color. The end result is a combination of mineralogical composition and firing temperature, as the briquettes have evidently shown. Future research on more combinations of mixed clays which will be fired at different temperatures will give further insight into this effect.

- Gajić-Kvašček, M.D, Marić-Stojanović, M.D, Jančić-Heinemann, R.M, Kvašček, G.S, and Dj Andrić, V (2012) Non-destructive characterisation and classification of ceramic artefacts using pEDXRF and statistical pattern recognition, *Chem. Central J.* 6, 102 (doi: 10.1186/1752-153X-6-102).
- Javanshah, Z (2018) Chemical and mineralogical analysis for provenancing of the Bronze age pottery from Shahr-i-Sokhta, South Eastern Iran. *SCIENTIFIC CULTURE*, Vol. 4, No 1, pp.83-92 (DOI: 10.5281/zenodo.1048247)
- Liritzis, I, Polymeris, G.S, Vafiadou, A, Sideris, A, Levy T.E (2018a) Luminescence dating of stone wall, tomb and ceramics of Kastrouli (Phokis, Greece) Late Helladic settlement: Case study. *Journal of Cultural Heritage* (in press) <https://doi.org/10.1016/j.culher.2018.07.009>
- Liritzis, I, Zacharias, N, Iliopoulos, I, Palamara, E, Xanthopoulou, V, Sideris, A, Vafiadou, A, Papageorgiou, I (2018b) Spectroscopy analysis for characterization and provenance of ceramic fabric and local clays from Late Helladic Kastrouli (Central Greece) (to be submitted for publication)
- Milotta F.L.M., Stanco F., Tanasi D. (2017) ARCA (Automatic Recognition of Color for Archaeology): A Desktop Application for Munsell Estimation. In: Battiato S., Gallo G., Schettini R., Stanco F. (eds) *Internat. Conf. Image Analysis and Processing - ICIAP 2017*. ICIAP 2017. 661-671, Lecture Notes in Computer Science, vol 10485. Springer, Cham. <http://iplab.dmi.unict.it/ARCA108/>
- Mantzourani, H and Liritzis, I (2006) Chemical analysis of pottery samples from Late Neolithic Kantou-Kouphouvounos and Sotira-Tepes. *Reports of Dept. of Antiquities Cyprus*, 63-76.
- Papageorgiou, I and Liritzis, I (2007) Multivariate mixture of normals with unknown number of components. An application to cluster Neolithic ceramics from the Aegean and Asia Minor. *Archaeometry* 49, 4, 795-813
- Soil Survey Manual (1951) Soil Survey Staff, U.S. Department of Agriculture Handbook, No.18, Washington D.C.
- Sideris, A, Ioannis Liritzis, Brady Liss, Matthew D. Howland, Thomas E. Levy (2017) At-risk cultural heritage: new excavations and finds from the Mycenaean site of Kastrouli, Phokis, Greece *Mediterranean Archaeology and Archaeometry*, Vol. 17, No 1, (2017), pp. 271-285
- Levy, T.E, Sideris, A, Howland, M, Liss, B, Tsokas, G, Stambolidis, A, Fikos, E, Vargemezis, G, Tsourlos, P, Georgopoulos, A, Papatheodorou, G, Garaga, M, Christodoulou, D, Norris, R, Rivera-Collazo, L, and Liritzis, I (2018) At-Risk World Heritage, Cyber, and Marine Archaeology: The Kastrouli-Antikyra Bay Land and Sea Project, Phokis, Greece, Springer International Publishing AG In T.E. Levy, I.W.N. Jones (eds.), *Cyber-Archaeology and Grand Narratives, One World Archaeology*, 143-230 (DOI 10.1007/978-3-319-65693-9_9).
- Xanthopoulou, V, Iliopoulos, I, Liritzis, I (2018) A detailed SEM-XRD analysis for characterization and provenance of ceramic fabric and local clays from Late Helladic Kastrouli settlement (to be submitted).

APPENDIX



Figure A1: Macro photo of all ceramics analyzed

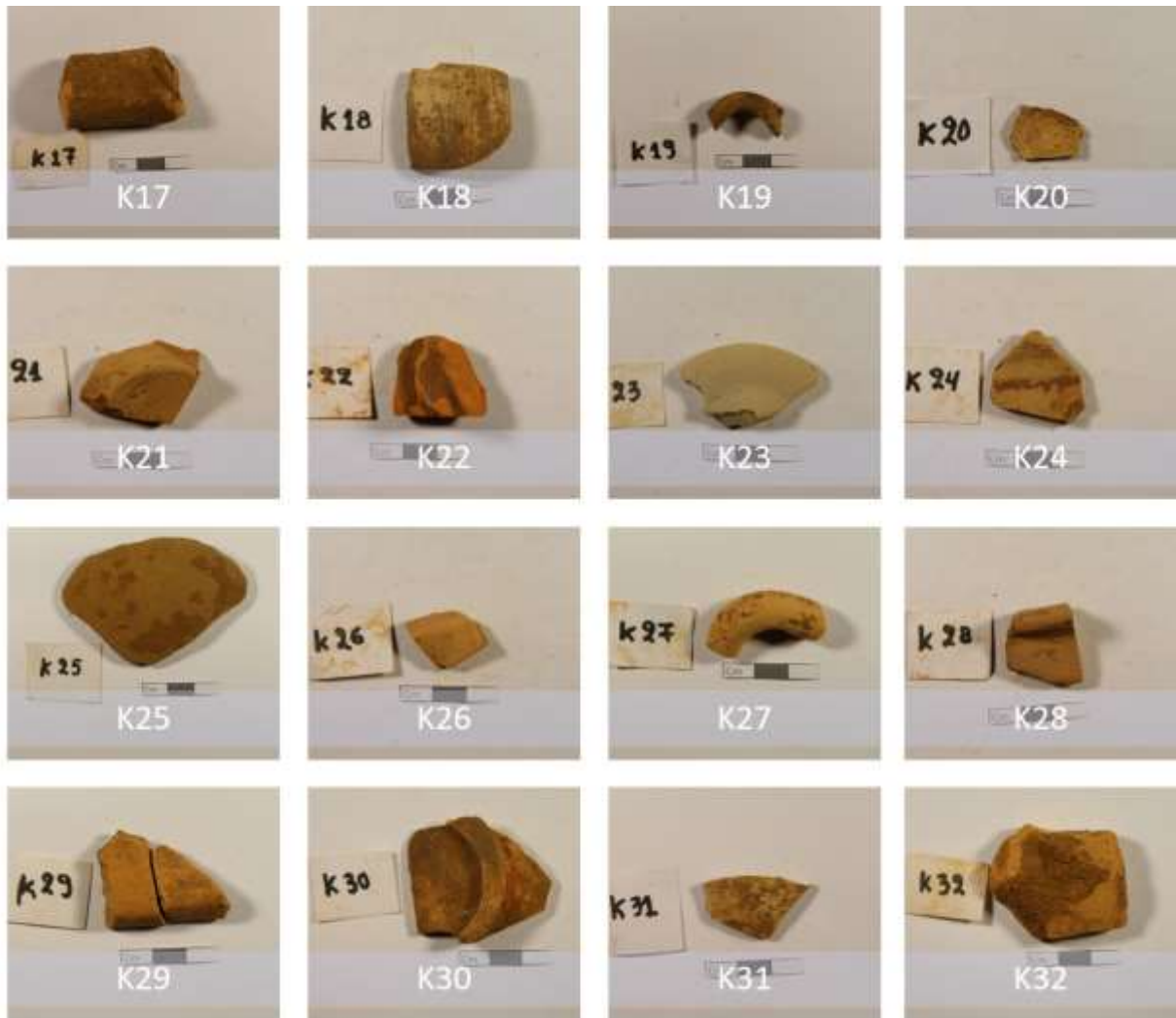


Figure A1 (continued)

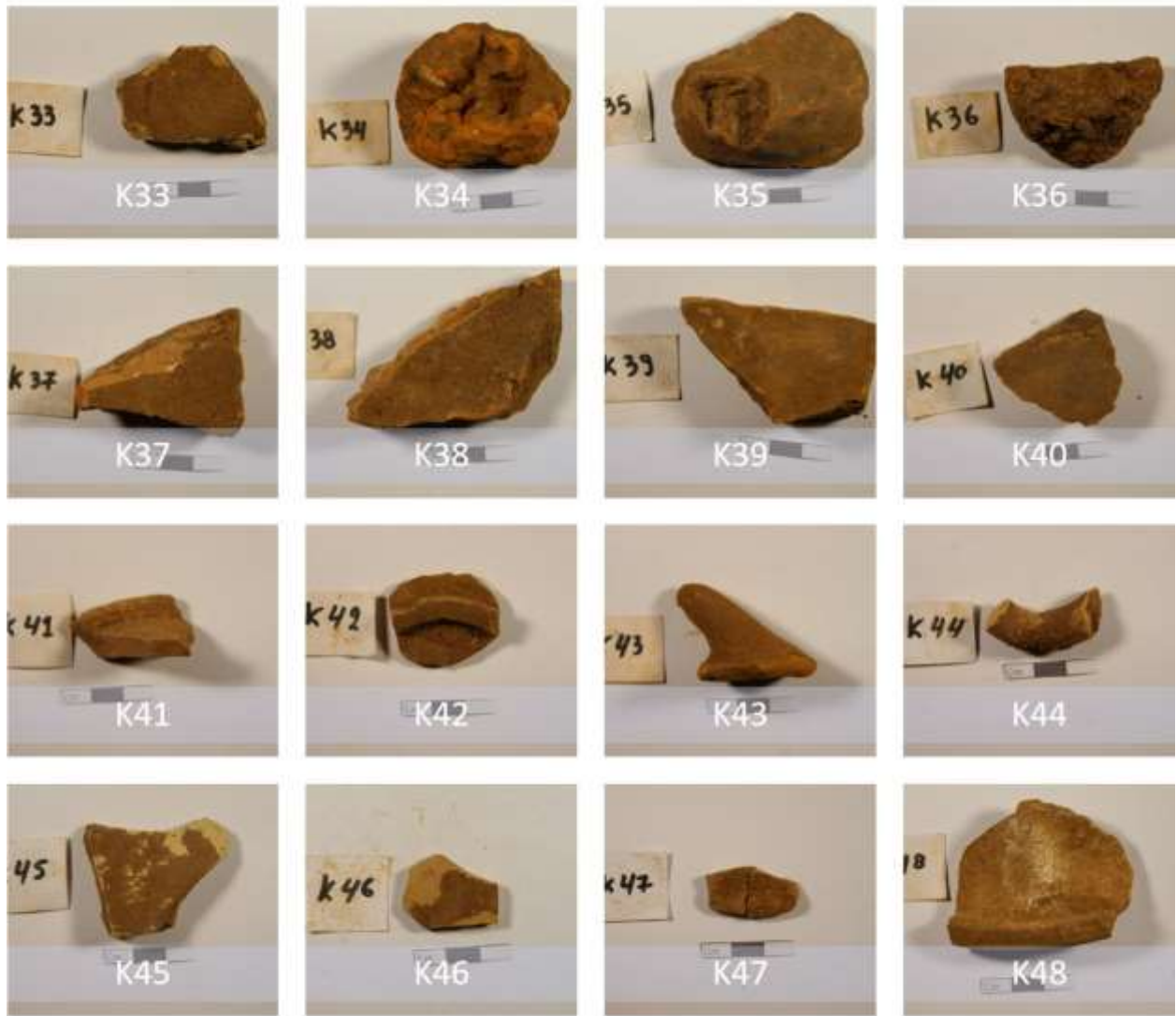


Figure A1 (continued)



Figure A1 (continued)



Figure A1 (continued)



Figure A1 (continued)



Figure A1 (continued)



Figure A1 (continued)

TABLE A1. All ceramic finds were grouped by the four users according to the Munsell scale.

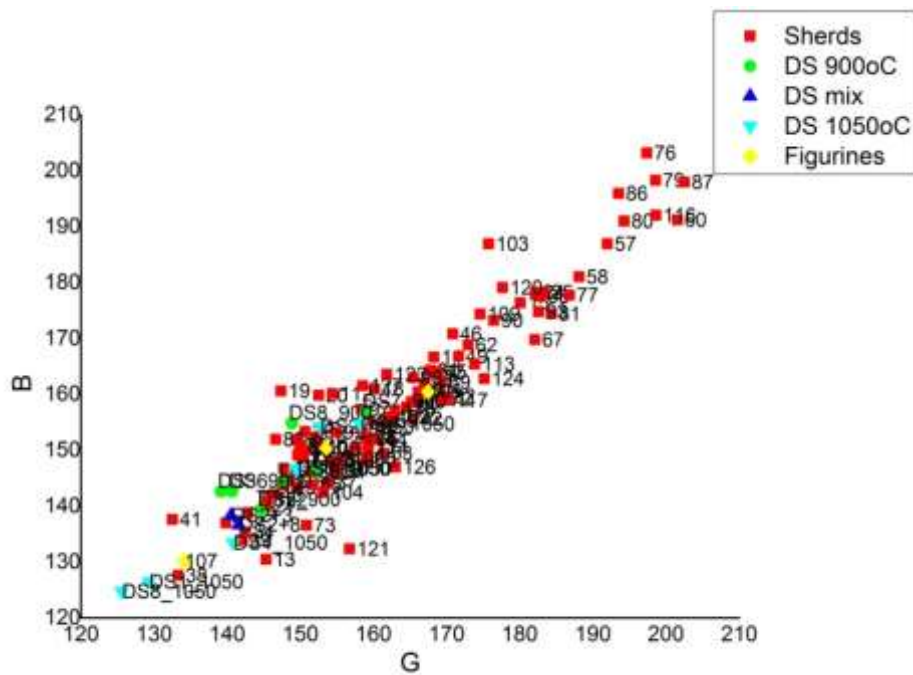
Samples		Vayia		Eleni		Maria		Asimina	
		Hue	Value/ Chroma	Hue	Value/ Chroma	Hue	Value/ Chroma	Hue	Value/ Chroma
K1	Inner layer	7.5YR	7/3	10YR	7/3	5YR	7/4	10YR	6/1
	Margin	2.5YR	5/4					7.5YR	7/3
K2	Inner layer	5YR	6/4	5YR	6/6	5YR	6/4	5YR	7/4
	Margin	2.5YR	5/8			5YR	6/6	2.5YR	6/6
K3	Inner layer	7.5YR	6/4	10YR	6/3	10YR	6/3	10YR	6/3
	Margin					10YR	5/3		
K4	Inner layer	7.5YR	4/6	10YR	7/1	2.5YR	7/1	2.5YR	7/1
	Margin	7.5YR	7/3						
K5		5YR	7/6	5YR	6/6	5YR	6/6	5YR	6/4
K6	Inner layer	2.5Y	4/1	2.5Y	4/1	5YR	4/1	5YR	4/1
	Margin	5YR	5/4			2.5YR	5/6		
K7	Inner layer	10YR	7/2	2.5Y	7/1	2.5YR	7/1	2.5Y	7/1
	Margin	7.5YR	8/4			10YR	7/3		
K8		10YR	7/4	10YR	6/4	10YR	6/3	10YR	7/3

K9		7.5YR	7/6	7.5YR	7/4	7.5YR	6/4	7.5YR	7/4
K10	Inner layer			10YR	6/4	10YR	6/2	10YR	6/3
	Margin	5YR	5/8			5YR	6/8		
K11		7.5YR	7/6	5YR	7/6	5YR	6/4	5YR	7/4
K12		5YR	6/6	5YR	7/4	5YR	7/4	5YR	6/4
K13		5YR	7/6	7.5YR	6/6	5YR	7/6	5YR	7/6
K14		5YR	7/6	5YR	6/6	5YR	6/6	5YR	7/6
K15		7.5YR	7/4	7.5YR	7/4	7.5YR	7/4	7.5YR	7/4
K16	Inner layer	2.5YR	6/8	7.5YR	6/4	5YR	6/6	5Y	5/1
	Margin	7.5YR	7/4						
K17		7.5YR	7/3	7.5YR	7/4	7.5YR	7/3	7.5YR	7/3
K18		10YR	8/3	10YR	7/3	10YR	6/3	10YR	7/2
K19		10YR	7/4	10YR	7/2	10YR	7/3	10YR	7/2
K20		10YR	7/4	10YR	8/3	10YR	8/3	10YR	7/2
K21		7.5YR	7/4	7.5YR	6/4	7.5YR	6/4	7.5YR	6/4
K22	Inner layer			2.5Y	6/1	5Y	6/1	5Y	6/1
	Margin	5YR	6/6	5YR	6/6	5YR	6/6	5YR	6/6
K23		2.5Y	7/4	2.5Y	7/3	2.5Y	8/2	2.5Y	8/2
K24		7.5YR	7/3	10YR	6/4	7.5YR	6/4	7.5YR	6/4
K25	Inner layer	5Y	6/1	2.5Y	6/2	5Y	7/1	2.5Y	8/1
	Margin	7.5YR	6/6						
K26		7.5YR	7/4	7.5YR	6/4	7.5YR	6/4	7.5YR	6/4
K27		7.5YR	8/4	7.5YR	7/4	7.5YR	7/4	7.5YR	7/4
K28		7.5YR	6/4	7.5YR	6/3	7.5YR	5/4	7.5YR	6/3
K29	Inner layer			10YR	7/4	7.5YR	6/6	10YR	6/3
	Margin	5YR	7/6			7.5YR	7/4	5YR	6/4
K30	Inner layer			10YR	7/3	5YR	6/2	7.5YR	8/3
	Margin	5YR	7/6			5YR	7/4	5YR	7/6
K31		2.5Y	7/2	2.5Y	8/2	10YR	7/2	2.5Y	7/1
K32	Inner layer	2.5Y	7/1	7.5YR	6/6	7.5YR	7/6	10YR	7/2
	Margin	7.5YR	6/6					5YR	7/6
K33	Inner layer					5Y	7/1	2.5Y	7/1
	Margin	10YR	7/4	10YR	7/1	7.5YR	8/2		
K34		5YR	6/8	5YR	5/8	5YR	6/6	5YR	6/6
K35	Inner layer	2.5Y	6/1	2.5Y	5/1	5YR	6/4	7.5YR	5/4
	Margin	2.5YR	5/8			5YR	5/3		
K36		5YR	6/4	5YR	5/8	5YR	6/4	5YR	6/4
K37		5YR	6/6	5YR	5/8	5YR	7/6	5YR	6/4
K38		5YR	5/6	5YR	5/8	5YR	5/6	5YR	7/2
K39		5YR	6/8	7.5YR	6/6	5YR	6/6	5YR	6/6
K40		5YR	6/6	7.5YR	6/8	5YR	7/6	5YR	6/6

K41		5YR	6/4	7.5YR	6/4	5YR	6/3	7.5YR	6/3
K42		7.5YR	7/4	10YR	6/4	7.5YR	6/4	7.5YR	7/3
K43		7.5YR	6/6	7.5YR	6/6	7.5YR	6/6	7.5YR	6/6
K44		7.5YR	8/6	7.5YR	7/4	7.5YR	7/4	7.5YR	7/4
K45		10YR	8/3	2.5Y	8/4	2.5Y	8/3	10YR	8/2
K46		7.5YR	6/4	10YR	6/4	7.5YR	7/4	7.5YR	7/4
K47	Inner layer	10YR	7/4			10YR	6/4	10YR	6/2
	Margin	2.5Y	6/2	2.5Y	7/2				
K48		7.5YR	7/4	7.5YR	7/4	7.5YR	7/3	7.5YR	7/3
K49		2.5Y	8/3	2.5Y	8/2	2.5YR	8/2	2.5Y	8/2
K50		10YR	8/2	2.5Y	8/3	2.5YR	8/2	2.5Y	8/2
K51	Inner layer	5YR	6/6	5YR	7/6	2.5YR	7/6	10YR	7/2
	Margin	5Y	7/2						
K52		10YR	7/3	10YR	7/3	5YR	7/6	7.5YR	7/3
K53		7.5YR	7/4	7.5YR	7/4	5YR	7/6	7.5YR	7/4
K54		5YR	7/6	5YR	6/4	5YR	7/6	5YR	6/4
K55	Inner layer	5YR	6/6	5YR	6/6			5YR	6/6
	Margin			7.5YR	7/4	7.5YR	7/4	7.5YR	6/4
K56		10YR	7/3	10YR	7/3	10YR	8/2	10YR	8/2
K57		2.5Y	8/2	2.5Y	8/2	5YR	8/1	2.5Y	7/2
K58		7.5YR	7/4	7.5YR	7/3	5YR	7/4	7.5YR	7/4
K59	Inner layer	5YR	5/6	7.5YR	6/6	5YR	6/6	5YR	6/6
	Margin	10YR	4/2						
K60		5YR	6/6	5YR	5/6	5YR	5/6	5YR	6/6
K61	Inner layer	5YR	5/1	5YR	6/8	2.5YR	6/8	2.5Y	6/1
	Margin	2.5YR	5/8	2.5Y	5/1			2.5YR	6/6
K62		5YR	6/8	5YR	6/6	5YR	6/6	5YR	6/6
K63		7.5YR	7/4	7.5YR	7/4	7.5YR	7/4	7.5YR	7/4
K64		10YR	8/3	2.5Y	8/2	10YR	8/2	10YR	8/2
K65		7.5YR	6/4	7.5YR	7/4	7.5YR	6/4	7.5YR	6/4
K66		2.5Y	8/4	2.5Y	8/2	2.5Y	8/2	2.5Y	7/2
K67		7.5YR	7/4	10YR	7/3	10YR	7/2	10YR	7/2
K68		10YR	7/4	10YR	8/3	10YR	7/3	10YR	7/2
K69		2.5Y	8/3	2.5Y	7/2	2.5Y	7/3	2.5Y	7/2
K70	Inner layer	5YR	6/8	5YR	6/6	10YR	6/3	7.5YR	7/3
	Margin			7.5YR	7/4	2.5YR	6/6	2.5YR	6/6
K71		10YR	7/4	7.5YR	7/4	7.5YR	7/4	7.5YR	7/3
K72		2.5YR	6/8	5YR	6/6	5YR	6/6	5YR	6/6
K73	Inner layer	2.5Y	5/1	2.5Y	5/1	10YR	8/2	10YR	5/1
	Margin	7.5YR	8/4						
K74		5YR	6/6	5YR	7/4	5YR	6/4	5YR	6/4

K75		5YR	6/4	5YR	7/4	5YR	6/4	7.5YR	6/2
K76		2.5Y	8/3	2.5Y	8/2	10YR	8/2	10YR	8/1
K77		10YR	8/4	10YR	8/4	10YR	8/3	10YR	7/3
K78		5YR	6/8	7.5YR	6/6	5YR	6/6	7.5YR	6/6
K79		2.5Y	8/2	2.5Y	8/2	2.5Y	7/3	2.5Y	8/1
K80		10YR	8/4	2.5Y	8/3	2.5Y	8/2	2.5Y	7/3
K81		10YR	7/4	10YR	7/4	10YR	7/3	10YR	8/3
K82		2.5YR	5/8	7.5YR	6/6	5YR	7/8	5YR	7/6
K83		2.5Y	6/1	5Y	6/1	7.5YR	7/4	2.5Y	6/1
K84		10YR	7/4	10YR	7/4	10YR	7/4	10YR	7/4
K85		2.5YR	6/8	5YR	6/8	5YR	6/6	5YR	6/8
K86		7.5YR	6/4	2.5Y	5/1	7.5YR	5/3	2.5Y	6/1
K87		10YR	8/4	10YR	8/3	10YR	7/3	10YR	7/3
K88		2.5YR	6/8	5YR	6/8	2.5YR	6/8	5YR	6/6
K89		5YR	6/6	5YR	6/6	2.5YR	6/4	5YR	7/6
K90		5YR	8/4	7.5YR	8/4	7.5YR	8/4	7.5YR	8/2
K91		7.5YR	7/6	7.5YR	7/3	7.5YR	7/4	7.5YR	7/4
K92		7.5YR	7/4	7.5YR	7/4	7.5YR	7/4	7.5YR	7/4
K93		7.5YR	7/6	7.5YR	7/4	7.5YR	6/4	7.5YR	7/4
K94		7.5YR	7/6	7.5YR	7/6	7.5YR	7/4	7.5YR	7/6
K95		5YR	6/8	5YR	6/6	2.5YR	6/6	5YR	6/6
K96		7.5YR	7/6	2.5YR	7/6	5YR	7/4	7.5YR	6/4
K97		10YR	8/4	10YR	8/1	5YR	8/1	2.5Y	8/1
K98		7.5YR	7/6	2.5YR	6/6	5YR	6/4	7.5YR	6/4
K99		2.5YR	6/8	7.5YR	8/6	5YR	6/4	7.5YR	7/4
K100	Inner layer	2.5YR	4/1	2.5Y	4/1	2.5YR	6/8	5YR	4/1
	Margin	2.5YR	6/8	2.5YR	6/8	10YR	4/1	2.5YR	6/6
K101		2.5YR	4/6	5YR	6/6	5YR	5/6	5YR	6/6
K102		7.5YR	7/6	7.5YR	7/6	7.5YR	7/4	7.5YR	7/4
K103		10YR	6/4	7.5YR	8/3	7.5YR	7/4	7.5YR	7/4
K104		5YR	6/6	7.5YR	6/6	5YR	6/6	5YR	7/6
K105				7.5YR	7/4	5YR	7/4		
K106				7.5YR	7/6	7.5YR	6/4		
K107				7.5YR	7/6	5YR	5/3		
K108				5YR	7/6	5YR	6/4		
K109		5YR	7/6	5YR	7/6	2.5YR	7/6	5YR	6/6
K110	Inner layer	10YR	5/1	2.5Y	5/1	5YR	6/3	2.5Y	5/1
	Margin	10YR	6/4	7.5YR	5/6			7.5YR	5/4
K111		10YR	6/6	10YR	7/6	10YR	7/6	10YR	7/6
K112		7.5YR	8/4	7.5YR	8/4	7.5YR	8/4	7.5YR	7/4
K113		7.5YR	7/6	7.5YR	7/6	7.5YR	7/4	7.5YR	7/4

K114		10YR	8/3	10YR	8/4	10YR	8/4	10YR	8/3
K115		10YR	7/4	2.5Y	8/2	10YR	7/3	2.5Y	7/2
K116		10YR	8/3	10YR	8/2	10YR	7/3	10YR	7/3
K117		10YR	8/4	10YR	8/4	10YR	8/3	10YR	8/2
K118	Inner layer	2.5Y	6/2	2.5Y	6/2	5YR	6/8	2.5Y	7/1
	Margin	2.5YR	5/8			10YR	6/1	5YR	5/3
K119	Inner layer			7.5YR	7/6			7.5YR	7/4
	Margin	5YR	6/6			5YR	7/6	5YR	7/6
K120		10YR	8/4	7.5YR	8/4	7.5YR	7/4	10YR	7/4
K121		5Y	4/2	metal		5Y	4/2	5Y	4/1
K122		7.5YR	6/6	7.5YR	6/6	7.5YR	6/6	7.5YR	6/4
K123	Inner layer	10YR	7/3	10YR	6/4	10YR	5/4	10YR	6/2
	Margin	5YR	5/4						
K124		10YR	7/4	10YR	7/4	10YR	6/4	10YR	7/4
K125		2.5YR	6/8	10YR	5/4	2.5YR	6/8	7.5YR	5/3
K126		7.5YR	5/4	2.5Y	5/1	7.5YR	5/4	10YR	6/1
K127	Inner layer	10YR	7/3	2.5Y	7/1	10YR	7/4	10YR	7/3
	Margin	7.5YR	7/4						
		10YR	7/1						



(A)

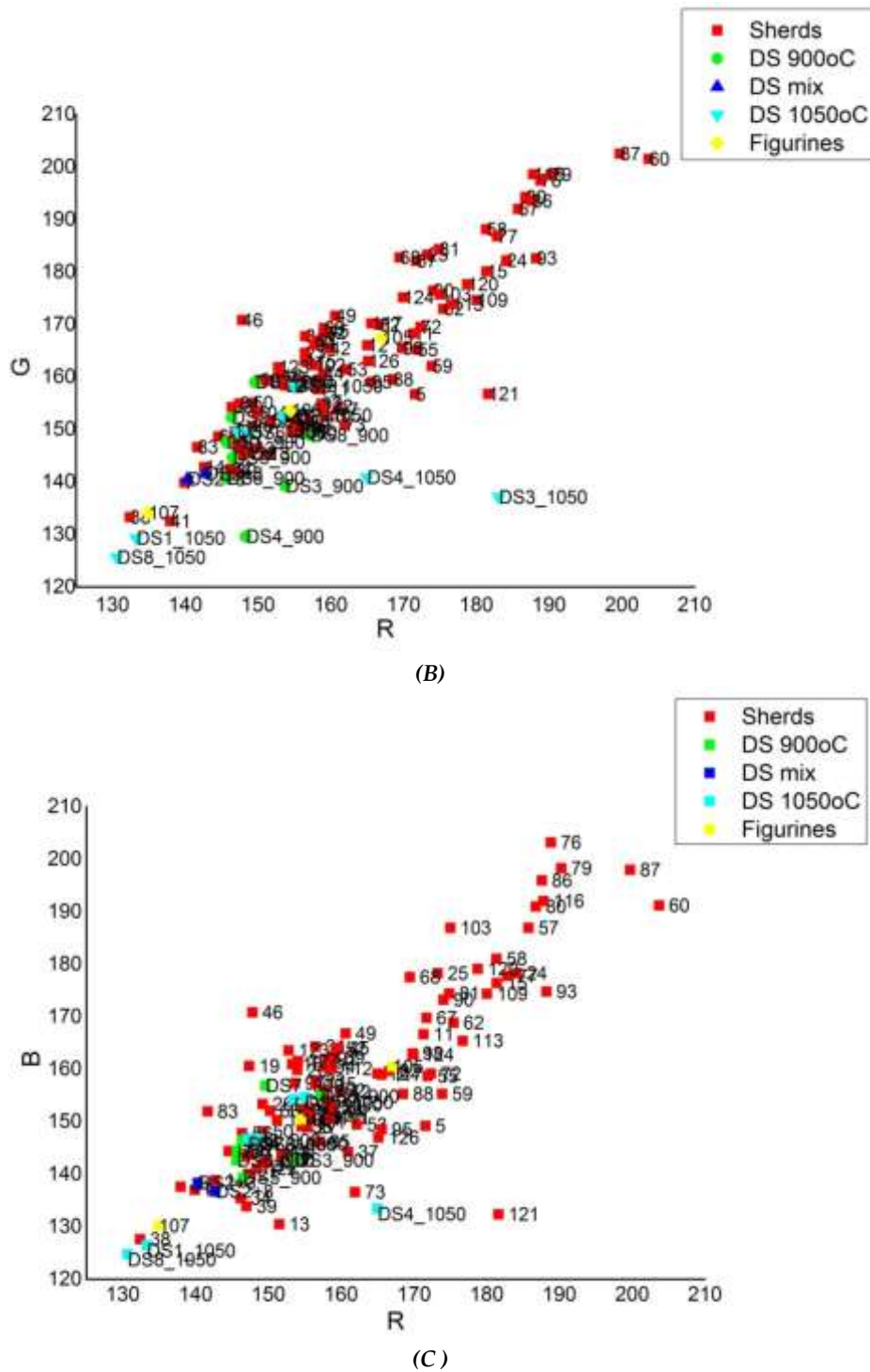


Figure A2: The three R-B, R-G and B-G projections for respective ceramic fabric and fired temperatures.

In Tables A2 and A3 some statistical data are presented, the mean values and the covariance matrix of R, G and B of the identified groups respectively, and a biplot of the averages with the standard error of the mean are given in Fig.A3.

Table A2. Mean values of R G B values for the three identified groups

	Group 1			Group 2			Group 3		
	R	G	B	R	G	B	R	G	B
mean	153	152	148	170	174	168	191	197	195

Table A3. Covariance matrices of the R G B values for the three identified groups

	Group 1			Group 2			Group 3		
	R	G	B	R	G	B	R	G	B
R	79	48	27	89	45	44	44	21	4
G	48	58	46	45	48	45	21	14	7
B	26	46	71	44	45	63	4	7	27

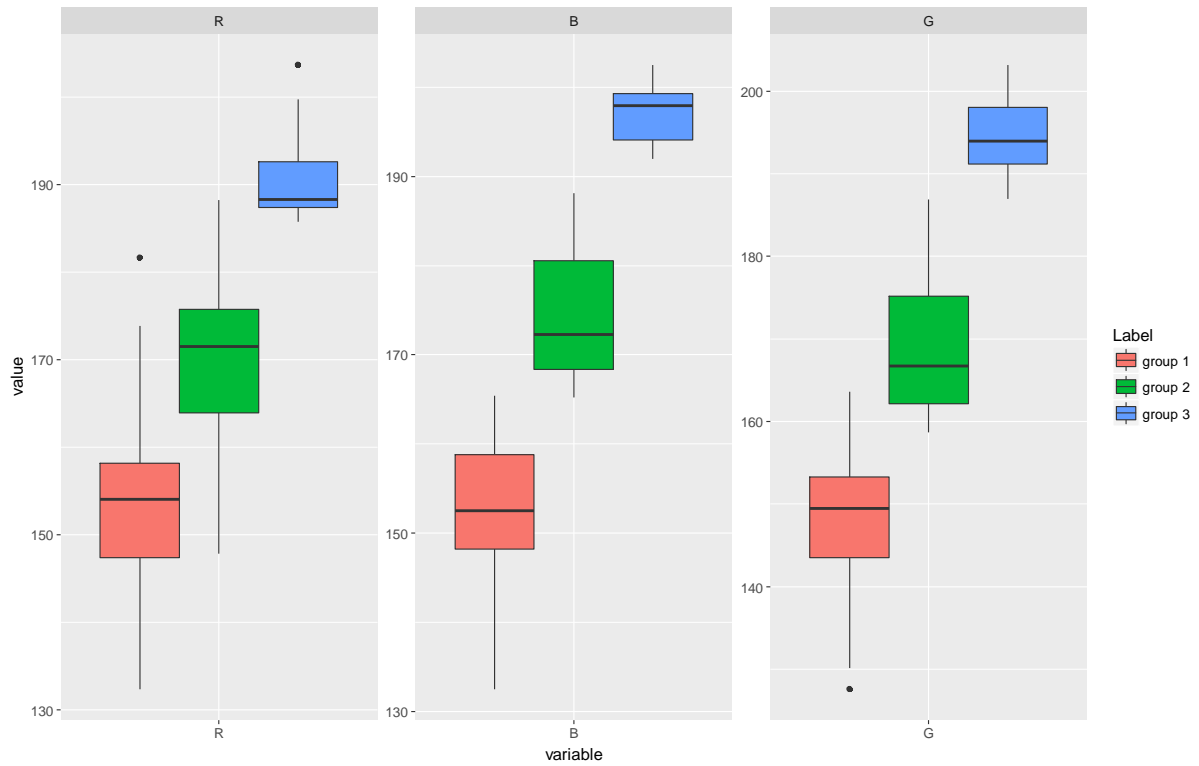


Figure A3. Boxplots of each variable by group as defined from cluster analysis in Fig.15.

It is apparent that group 1 has the lowest values in all 3 variables, group 2 moderate and group 3 the highest values on R, G and B.